

LA-UR-21-24482

Approved for public release; distribution is unlimited.

Title: CERBERUS: CEDT Phase-1 Preliminary Design for Cu Critical Experiment

Author(s): Amundson, Kelsey Marie
Cutler, Theresa Elizabeth
Little, Robert J.
Goda, Joetta Marie
Hutchinson, Jesson D.
Kawano, Toshihiko
Thompson, Nicholas William
Zerkle, M.
Sobes, V.
McDonnell, J. D.

Intended for: Report

Issued: 2021-06-29 (rev.2)

Disclaimer:

Los Alamos National Laboratory, an affirmative action/equal opportunity employer, is operated by Triad National Security, LLC for the National Nuclear Security Administration of U.S. Department of Energy under contract 89233218CNA000001. By approving this article, the publisher recognizes that the U.S. Government retains nonexclusive, royalty-free license to publish or reproduce the published form of this contribution, or to allow others to do so, for U.S. Government purposes. Los Alamos National Laboratory requests that the publisher identify this article as work performed under the auspices of the U.S. Department of Energy. Los Alamos National Laboratory strongly supports academic freedom and a researcher's right to publish; as an institution, however, the Laboratory does not endorse the viewpoint of a publication or guarantee its technical correctness.

IER 537: Copper Critical Experiment

CERBERUS: CEDT Phase-1 Preliminary Design for Cu Critical Experiment

Authors: Kelsey Amundson, Theresa Cutler, Robert Little, Joetta Goda, Jesson Hutchinson, Toshihiko Kawano, Jordan McDonnell, Vlad Sobes, Nicholas Thompson, Mike Zerkle

1.0 OBJECTIVE

The goal of the Critical Experiment Reflected By copper to better Understand Scattering [CERBERUS] is to design a critical experiment that maximizes sensitivities to Cu reactions, particularly in the intermediate energy region (0.625 eV – 100 keV). Despite the number of experiments evaluated in the International Criticality Safety Benchmark Evaluation Project (ICSBEP) Handbook¹, there is still a gap of benchmarks sensitive to neutrons in the intermediate energy region. Of the ICSBEP benchmarks sensitive to neutrons in the intermediate energy region, very few are also sensitive to Cu in that region. One of the primary intermediate energy benchmark evaluations is the ZEUS series, which uses a Cu reflector. However, concerns have been brought up about the nuclear data associated with Cu scattering in the reflector. Improving Cu nuclear data is important outside of the ZEUS series, because it is present in many bronze and aluminum alloys, which are used in various nuclear operations.

Recently, there has been a lot of work on Evaluated Nuclear Data Files (ENDF) that helped lead to improvements in the C-E values for the ZEUS series. However, studies performed by Robert Little² show that the majority of that improvement came from updates in ²³⁵U cross-sections. Therefore, an experiment focusing on Cu cross-sections, particularly Cu elastic scattering, will make the ZEUS benchmark series more useful for code and nuclear data validation.

The design criteria for this critical experiment series is: 1) maximizing sensitivity to Cu elastic scattering cross sections and angular distributions, 2) targeting the intermediate energy region for the neutron flux and Cu elastic scattering sensitivity, and 3) using materials with well-known nuclear data so Cu sensitivities can be better isolated. This report will provide a preliminary design that meets these criteria and the methodology for determining that design.

2.0 NUCLEAR DATA NEED

There is a need for improved Cu nuclear data in order to resolve concerns surrounding the ZEUS benchmark series. Efforts have been made to try to improve Cu cross-section data, but given that there are few benchmarks sensitive to Cu, a new experiment is needed.

¹ *International Handbook of Evaluated Criticality Safety Benchmark Experiments* / Nuclear Energy Agency. - Paris : OECD Nuclear Energy Agency, 2016. (NEA;7328).

² T. Cutler, J. Hutchinson, R. Little. *NCSP IER 489 CED-3a Documentation*, Los Alamos National Laboratory, 2019.

2.1. Copper Cross-Sections

Evaluated nuclear data for copper has been continuously revised in the past decades. ENDF/B-V provided nuclear data for natural copper. Starting with ENDF/B-VI.0, isotopic evaluations of ^{63}Cu (69.17 atom %) and ^{65}Cu (30.83 atom %) have been provided. The Cu isotopes were updated a total of four times as part of ENDF/B-VI for various reasons, appearing in ENDF/B-VI.0, ENDF/B-VI.2, ENDF/B-VI.6, and ENDF/B-VI.8. There were no substantive updates to Cu evaluated data in either ENDF/B-VII.0 or ENDF/B-VII.1. However, the ENDF/B-VII.0 “Big Paper”³ included the following information specific to data testing results for ZEUS:

“The graphite-moderated Zeus experiments, HEU-MET-INTER-006 were designed specifically to test the accuracy of ^{235}U cross sections in the intermediate energy range ... the bias between the benchmark values for k_{eff} and the values computed with ENDF/B-VII.0 decreases monotonically as the fraction of fissions in the intermediate energy range increases. This behavior, which also was observed with ENDF/B-VI, strongly suggests an energy-dependent bias in the ^{235}U cross sections over that range, which therefore requires further study in the future.

The unmoderated Zeus experiment, HMF-073, represents an upper-energy endpoint for the Zeus experiments discussed ... ENDF/B-VII.0 calculations for this benchmark over predict k_{eff} by more than 1%. However, when ENDF/B-V cross sections for copper are used, the calculated value for k_{eff} is well within the experimental uncertainty for the benchmark. No such changes are seen for the graphite-moderated benchmarks, which have intermediate spectra. Consequently, this behavior strongly suggests that improvements are still needed in the copper cross sections in the fast neutron energy range.”

Based off the results from the ENDF/B-VII.0 “Big Paper”, the faster end of the intermediate region became the focus, since it was a challenge to cover the entire intermediate energy region. Significant attention was paid to the Cu isotopes for ENDF/B-VIII.0. See pages 20-24 of the ENDF/B-VIII.0 “Big Paper”⁴ for details of the new Cu evaluations. As mentioned earlier, data testing results specific for ZEUS indicated improved agreement with experiment when using ENDF/B-VIII.0, with the majority of that improvement deriving from updates made to the ^{235}U evaluation.

When examining a broader suite of criticality benchmarks that include Cu, a recent report by Shaw, et.al.⁵ concluded that the ENDF/B-VIII.0 changes to ^{63}Cu provided overall improved agreement with experiment, while the ENDF/B-VIII.0 changes to ^{65}Cu provided overall lessened agreement with experiment. The report noted that several ZEUS cases remained outliers.

³ M.B. Chadwick, P. Obložinský, M. Herman, et al., "ENDF/B-VII.0: Next Generation Evaluated Nuclear Data Library for Nuclear Science and Technology," Nuclear Data Sheets, Volume 107, Issue 12, 2006, Pages 2931-3060.

⁴ D.A. Brown, M.B. Chadwick, R. Capote, et al., "ENDF/B-VIII.0: The 8th Major Release of the Nuclear Reaction Data Library with CIELO-project Cross Sections, New Standards and Thermal Scattering Data," Nuclear Data Sheets, Volume 148, 2018, Pages 1-142.

⁵ Alex Shaw, Farzad Rahnema, Andrew Holcomb & Doug Bowen, "Validation of Continuous-Energy ENDF/B-VIII.0 ^{16}O , ^{56}Fe , and $^{63,65}\text{Cu}$ Cross Sections for Nuclear Criticality Safety Applications," Nuclear Science and Engineering, 195:4, 412-436 (2021).

Several aspects of Cu nuclear data have been mentioned as areas where improvement could be possible. These include elastic scattering angular distributions, structure in inelastic scattering cross sections, more accurate resonance parameters (including spin assignments), and capture cross sections.

2.2. Existing Benchmarks

As mentioned previously, very few ICSBEP benchmarks are sensitive to Cu in the intermediate energy region. Database for ICSBEP (DICE⁶) includes a repository of ICSBEP benchmarks and their sensitivities, which can be searched to find benchmarks that are sensitive to a certain reaction within an isotope. While nuclear data libraries change, a benchmark's sensitivity to a certain reaction does not vary significantly between cross-section libraries. Figure 1 shows a heat map of the total number of ICSBEP benchmarks sensitive to various Cu neutron reactions and almost all of the benchmarks are in the fast or thermal region, based on sensitivity data from the ICSBEP and DICE databases. A majority of the ICSBEP benchmarks sensitive to Cu reactions (e.g. total, capture, elastic, and inelastic) use uranium as a fuel. While these benchmarks are sensitive to Cu reactions, they were not designed to focus on Cu reactions and their effects.

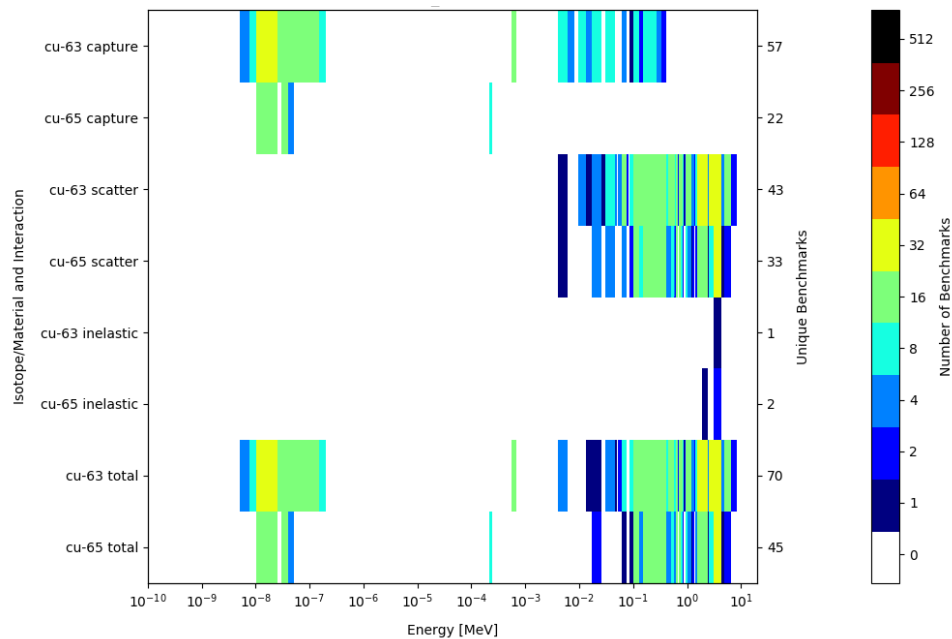


Figure 1: Heat map of the total number of ICSBEP benchmarks that are sensitive to Cu based on sensitivity data from the ICSBEP and DICE databases.

⁶ DICE: User's Manual, Nuclear Energy Agency. - Paris : OECD Nuclear Energy Agency, 2019.

2.3. ZEUS Series

In order to better understand the impact of ENDF/B-VII.1⁷ and ENDF/B-VIII.0⁸ cross-sections for ⁶³Cu and ⁶⁵Cu, various cross-section library combinations were tested for the ZEUS HMI-006 benchmark cases (1 through 4). The primary metric for this analysis is the trend of C-E between the configurations. In addition to the ENDF cross-sections, new libraries were made by V. Sobes and T. Kawano. The Sobes files for ⁶³Cu and ⁶⁵Cu for this report were generated through an optimization study of four ZEUS benchmark models. The angular distributions were optimized below 300keV to minimize the chi-squared metric of C/E in SCALE/KENO models using ENDF/B-VII.1 cross section libraries. The Toshihiko Kawano (TK) files used for test calculations were simple trial files that either increased or decreased the P1 values for elastic scattering by 10% over the incident neutron range from 0 - 1 MeV. The 10% value was a test scenario and not based off any other data. Table 1 and Figure 2 show the results of this analysis. It can be seen that ENDF/B-VIII.0 always performs better than ENDF/B-VII.1 and a better understanding of the scattering distributions will improve the agreement with the experiment.

Table 1: Cross-section library combinations for ZEUS HMI-006 configurations. The cross-section library listed in column 2 is the library used for all materials, except Cu, while the cross-section libraries listed in column 3 and 4 are the ENDF libraries used for ⁶³Cu and ⁶⁵Cu.

Variant	Cross-Section Library	⁶³ Cu	⁶⁵ Cu
1	ENDF7.1	7.1	7.1
2	ENDF7.1	8.0	7.1
3	ENDF7.1	7.1	8.0
4	ENDF7.1	8.0	8.0
5	ENDF8.0	8.0	8.0
6	ENDF8.0	7.1	8.0
7	ENDF8.0	8.0	7.1
8	ENDF8.0	7.1	7.1
9	ENDF8.0	Sobes	Sobes
10	ENDF8.0	TK_+10pct	TK_+10pct
11	ENDF8.0	TK_-10pct	TK_-10pct

⁷ J. Conlin, D. Parsons, et. al., *Continuous Energy Neutron Cross Section Data Tables Based upon ENDF/B-VII.1*, Los Alamos National Laboratory, LA-UR-13-20137, 2013.

⁸ J. Conlin, W. Haek, et. al., *Release of ENDF/B-VIII.0-Based ACE Data Files*, Los Alamos National Laboratory, LA-UR-1824034, 2018.

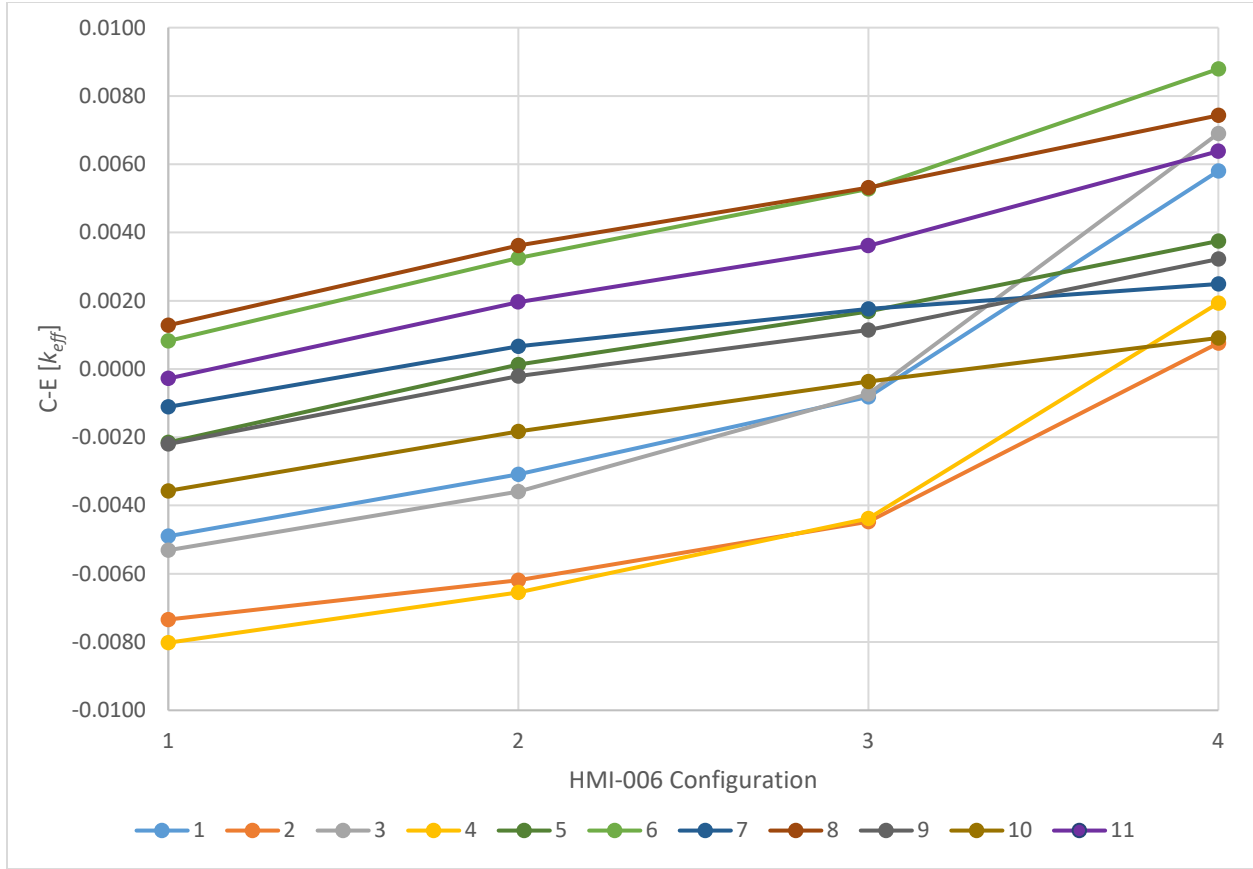


Figure 2: C-E Trend for ZEUS HMI-006 configurations for different cross-section library combinations.

3.0 DESIGN METHODOLOGY

All neutron transport calculations presented in this report were performed using MCNP6®⁹ particle transport code and ENDF/B-VIII.0 cross-section libraries. Reactions with the largest k_{eff} sensitivities are reported for the best configuration of each geometry and interstitial material. On each of the figures the energy-integrated KSEN sensitivity ($S_{k_{eff},x}$) is shown. This value is calculated as the partial derivative of k_{eff} divided by k_{eff} over the partial derivative of some nuclear data (isotope, reaction pair, etc.) divided by that nuclear data (see the equation below).

$$S_{k_{eff},x} = \frac{\partial k_{eff}/k_{eff}}{\partial x/x}$$

⁹ MCNP® and Monte Carlo N-Particle® are registered trademarks owned by Triad National Security, LLC, manager and operator of Los Alamos National Laboratory. Any third party use of such registered marks should be properly attributed to Triad National Security, LLC, including the use of the ® designation as appropriate. Any questions regarding licensing, proper use, and/or proper attribution of Triad National Security, LLC marks should be directed to trademarks@lanl.gov.

3.1. Design Descriptions

Multiple configurations were investigated to see if the calculated sensitivities matched the experiment criteria. Since ZEUS is already one of the most widely used intermediate energy benchmark series, a similar design was used as a starting point. Two geometries were investigated as part of the CED-1 design process. The initial two designs used 53.34cm diameter HEU plates (i.e. the Jemima plates) with repeating units surrounded by a reflector. The material composition of the Jemima plates can be seen in Table 2. The 53.34cm diameter plates involve using both the inner and outer Jemima plates, while using only the inner Jemima plates would lead to a diameter of 38.10cm. In both of these configurations, the core and reflector regions are cylindrical.

The first configuration, base, includes Cu as the only interstitial material. The second configuration, base+, includes Cu and another interstitial material that was changed throughout the design process. The only difference between the base and base+ case is that the base+ case has a second interstitial material. Images of two units within the base and base+ cores can be seen in Figure 3. The additional interstitial material was added to base+ in an effort to soften the neutron spectrum and make it an intermediate system, since systems with Cu as the only interstitial material result in fast systems. All design configurations use pure, metal Cu with natural isotopic abundances (as seen in Table 2).

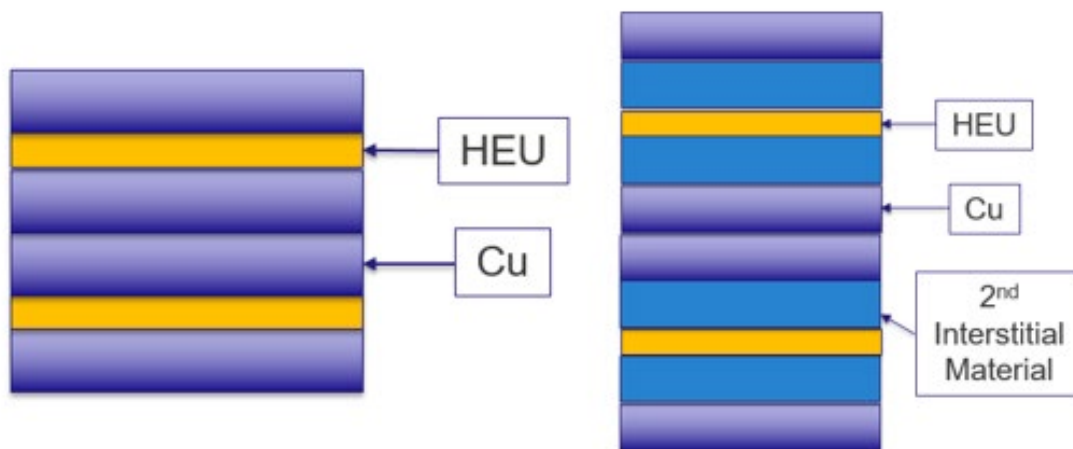


Figure 3: Example of 2 units of base (left) and base+ (right)

Table 2: Material definition of Jemima HEU plates and Cu interstitial and reflector for all configurations.

Jemima Definition¹⁰	
Density [g/cm³]	18.39
²³⁵U Atom Fraction	0.93
²³⁸U Atom Fraction	0.07
Cu Definition^{11,12}	
Density [g/cm³]	8.96
⁶³Cu Atom Fraction	0.6917
⁶⁵Cu Atom Fraction	0.3083

Simulations were performed where the interstitial materials in base and base+ were varied from 0.1 cm to 6.0 cm thicknesses. In addition, the effectiveness of both Cu and polyethylene (poly) reflectors were investigated in the base configuration. Studies on the thickness of the reflector were also performed, varying the reflector thicknesses from 0.1 cm to 30 cm. All of the initial studies use a core with five, vertically stacked units, but were re-evaluated with a critical configuration. Additional units were added after the initial configurations were down-selected in order to assess the feasibility of creating a critical experiment. To ensure that a designed experiment goes critical during execution of the experiment, a simulated k_{eff} greater than one is used. An ideal simulated $k_{\text{eff}} \sim 1.02$, since there are simplifications included in the models and a larger value allows for some unknowns in cross-section data. Most simplifications will be removed during final experiment design (CED-2).

3.2. Base

As mentioned in Section 3.1, base only uses HEU and Cu plates in the core. The base core has a total of 15 unique core configurations. The differences between these configurations is the thickness of the Cu interstitial. The HEU plates are already within the NCERC inventory, so the fuel thickness does not need to be varied. During the analysis of base, the effectiveness of a 30cm poly reflector vs. a 30cm Cu reflector was investigated for all base core configurations. The effect of reflector thickness was also investigated for all base core and reflector material configurations. A sample input for base can be found in Appendix D.

3.2.1. Varying Reflector Material

Cu was one of the reflector materials considered because it is the reflector material used in the ZEUS benchmark series and natural copper was chosen for simplicity in modeling. Poly was chosen as the other reflector material to investigate because of its high scattering cross-section and its well-known nuclear data. The material definition for the poly reflector, and all other poly components in other geometries, is shown in Table 3. Figure 4 shows how the reflector material

¹⁰ HEU-MET-FAST-073, HEU-MET-FAST-072, and HEU-MET-INTER-006

¹¹ Natural Abundance: <https://www.webelements.com/copper/isotopes.html>

¹² Density: <https://www.lenntech.com/periodic-chart-elements/density.htm>

and Cu interstitial thickness affects k_{eff} . Note, none of the initial configurations are close to critical, but this does show how the trend changes between the different reflector materials and as Cu interstitial thickness is increased.

Table 3: Material Definition of Poly Interstitial and Reflector for All Configurations.

Poly Definition ¹³	
Density [g/cm ³]	0.93
¹ H Atom Density [at/b-cm]	8.24145*10 ⁻²
² H Atom Density [at/b-cm]	1.23640*10 ⁻⁵
¹² C Atom Density [at/b-cm]	4.12154*10 ⁻²

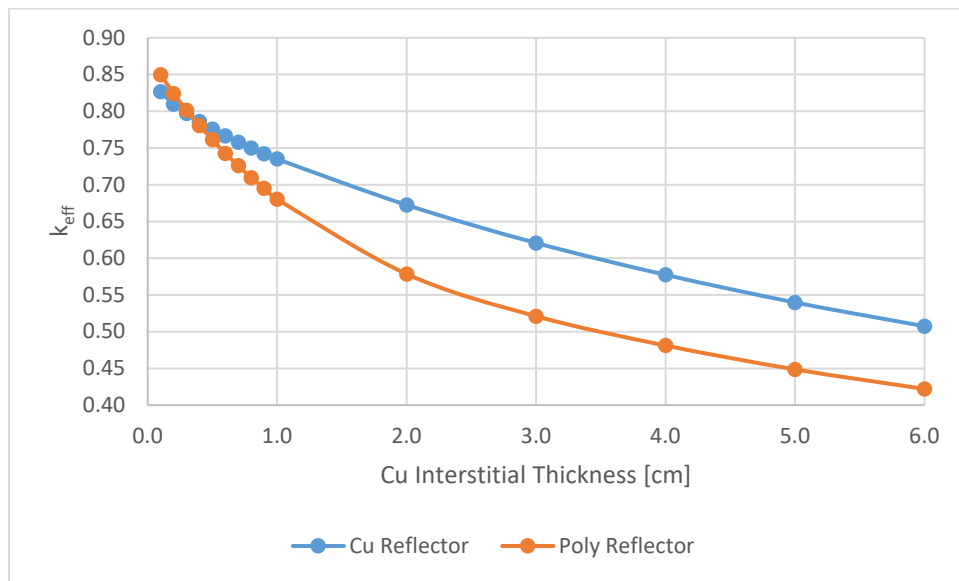


Figure 4: The change in k_{eff} as the Cu interstitial layers increase in thickness for Base. All configurations displayed are 5 units and have a 30cm reflector.

In Figure 4, when the Cu interstitial thickness reaches 0.4 cm thick, the Cu reflector has a higher k_{eff} than the poly reflector. This occurs because the addition of poly leads to more scattering events in the reflector, resulting in significant neutron thermalization, which eventually leads to more capture events and takes away neutrons that could fission.

In order to determine if any of the configurations under base meet the experiment criteria, sensitivity profiles were analyzed. ⁶³Cu and ⁶⁵Cu have similar sensitivity profile shapes, but are different magnitudes. Therefore, only ⁶³Cu sensitivities are displayed in this report. In addition to

¹³ Density & chemical formula: <https://omnexus.specialchem.com/selection-guide/polyethylene-plastic>. Note, there are a range of densities for polyethylene, so a value that is included in the high-density and low-density ranges was chosen. The material card definition was calculated from the chemical composition.

showing Cu scattering sensitivities, ^{235}U total nu sensitivities will be shown, which shows the sensitivity to the distribution of neutrons causing fissions. Figures 5-7, show how the sensitivities to ^{63}Cu elastic, ^{63}Cu (n, γ), and ^{235}U total nu change as the Cu interstitial thickness increases.

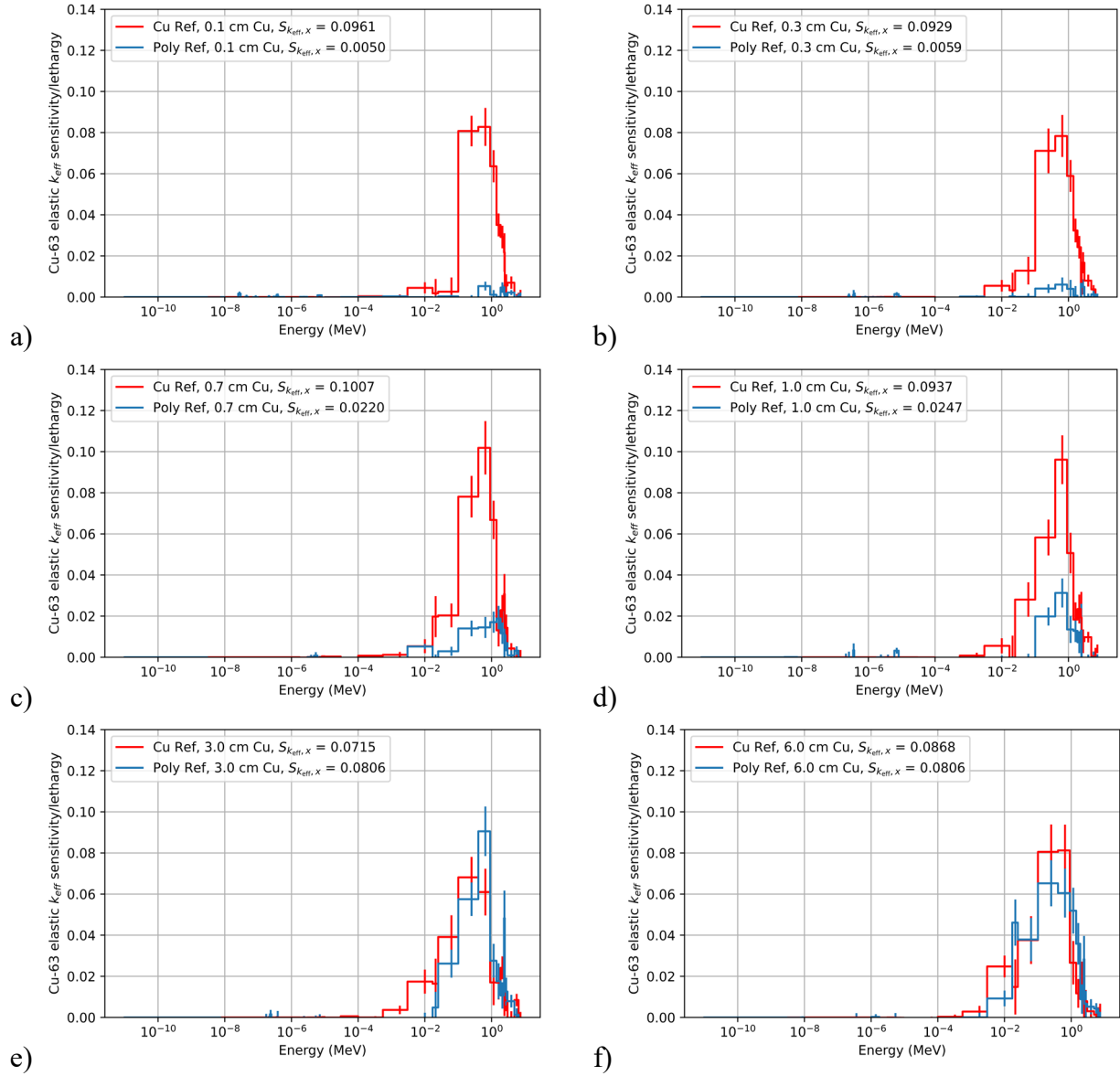


Figure 5: Compares ^{63}Cu elastic scattering sensitivities between 30 cm Cu (red) and Poly (blue) reflectors for Cu interstitial thicknesses of a) 0.1 cm, b) 0.3 cm, c) 0.7 cm, d) 1.0 cm, e) 3.0 cm, and f) 6.0 cm. All configurations only include 5 units.

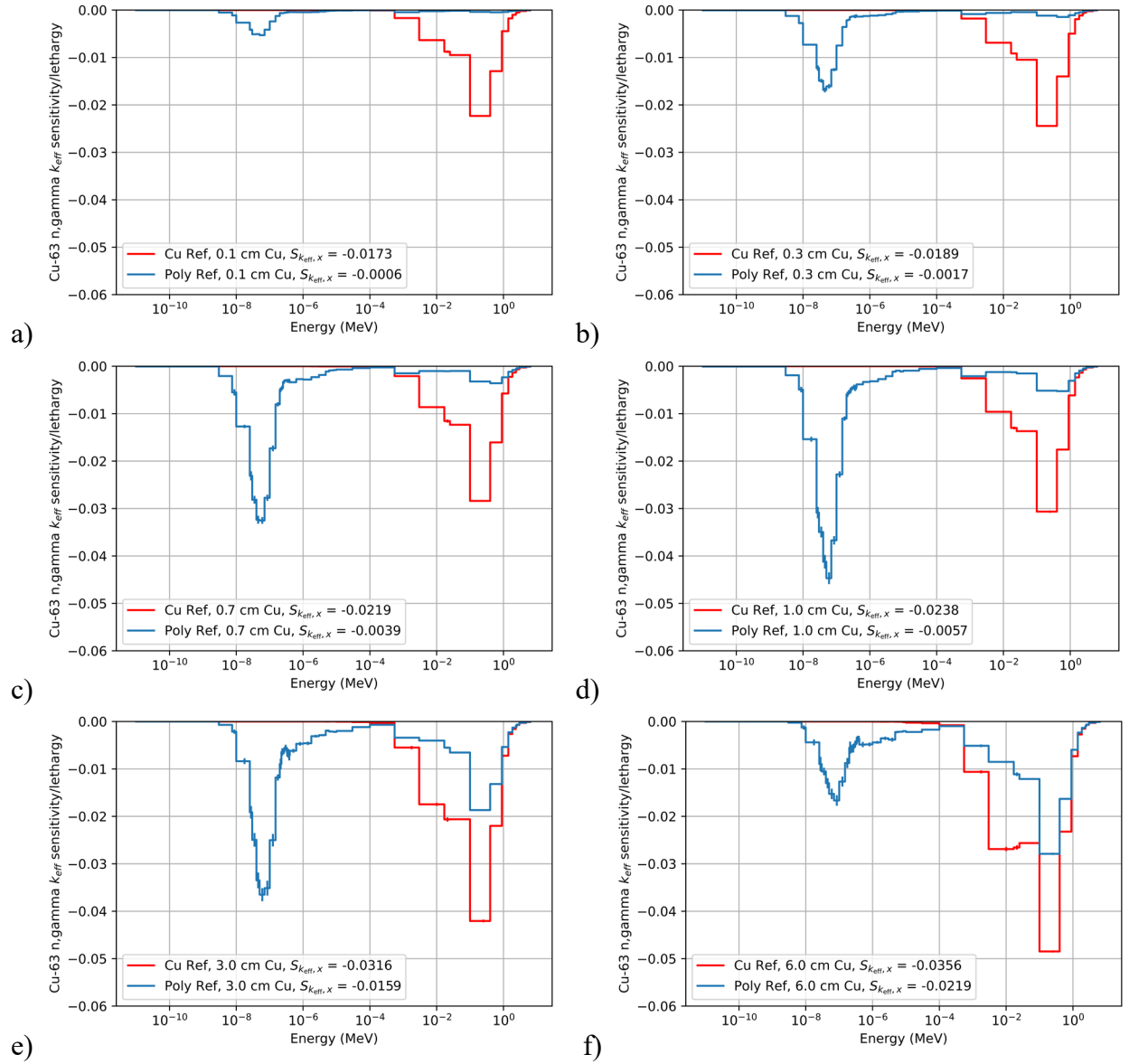


Figure 6: Compares ^{63}Cu (n, γ) sensitivities between 30 cm Cu (red) and Poly (blue) reflectors for Cu interstitial thicknesses of a) 0.1 cm, b) 0.3 cm, c) 0.7 cm, d) 1.0 cm, e) 3.0 cm, and f) 6.0 cm. All configurations only include 5 units.

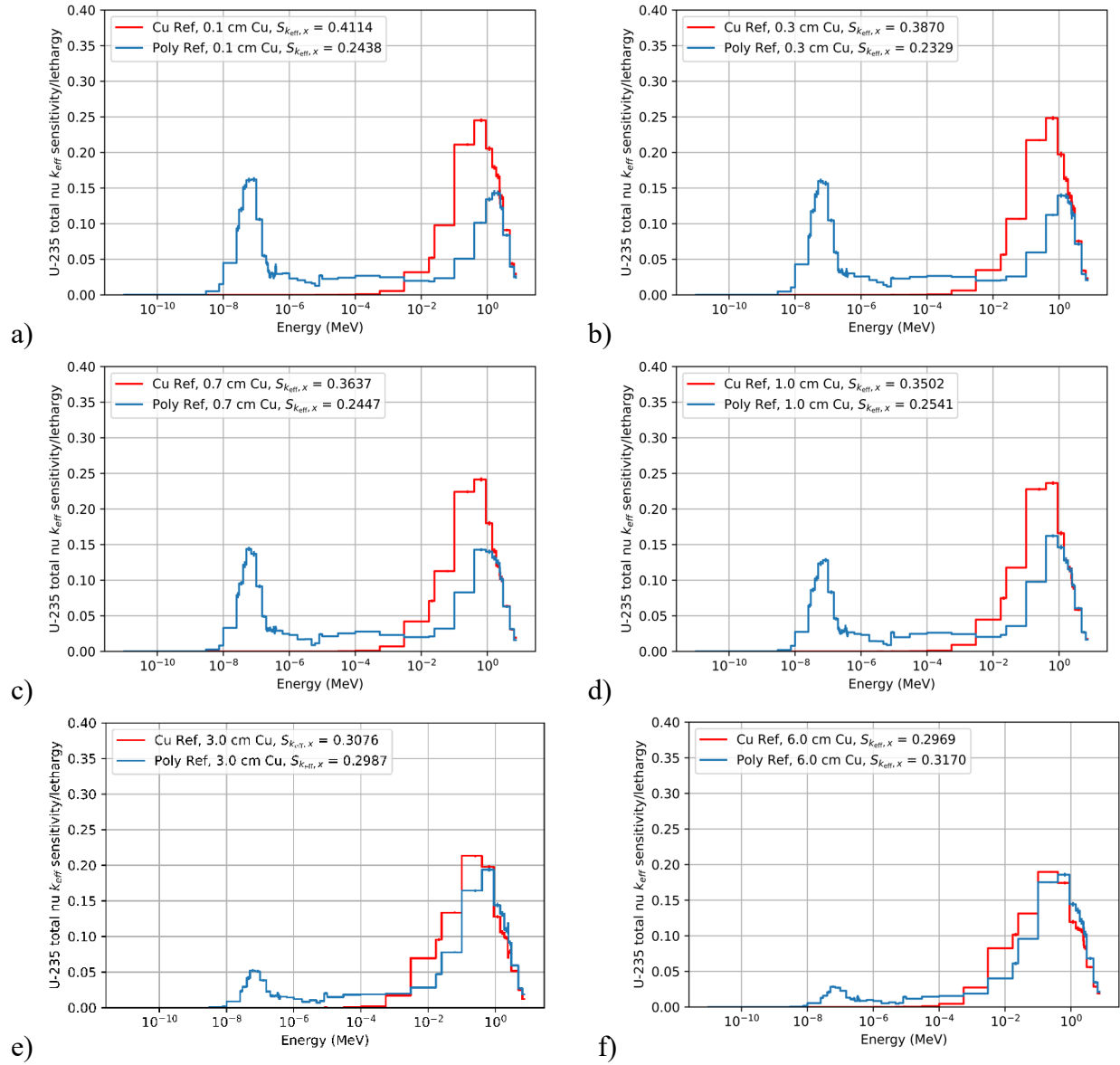


Figure 7: Compares ^{235}U total nu sensitivities between 30 cm Cu (red) and Poly (blue) reflectors for Cu interstitial thicknesses of a) 0.1 cm, b) 0.3 cm, c) 0.7 cm, d) 1.0 cm, e) 3.0 cm, and f) 6.0 cm. All configurations only include 5 units.

Based off the sensitivity profiles, the poly reflector does not help achieve an intermediate energy system or help increase the sensitivity to Cu elastic scattering. Therefore, the IER team decided to only focus on configurations using a Cu reflector. The sections that follow build upon this decision.

3.2.2. Varying Reflector Thickness

The next component to vary was the reflector thickness. Since, Section 3.2.1 concluded that a poly reflector would not contribute to meeting the design criteria, only the results for varying Cu reflector thickness are reported. Figure 8 shows how varying the reflector thickness affects k_{eff} for a subset of Cu interstitial thicknesses.

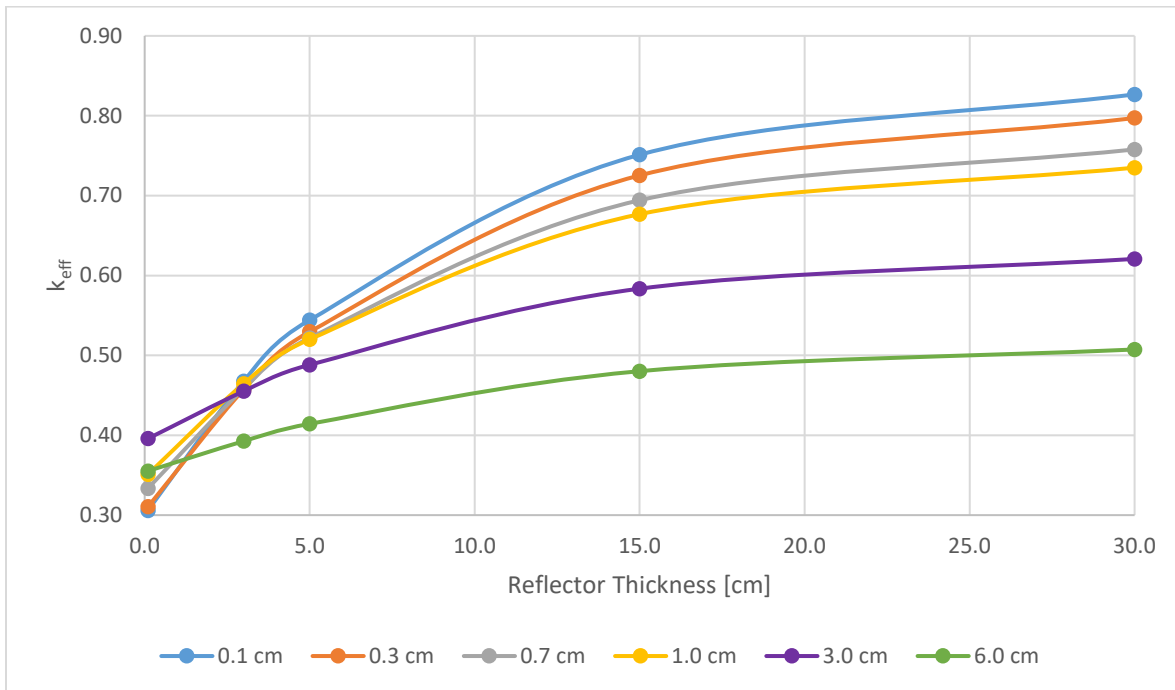


Figure 8: Change in k_{eff} as reflector thickness changes for various Cu interstitial thicknesses (0.1, 0.3, 0.7, 1.0, 3.0, and 6.0 cm). All configurations only include 5 units.

The sensitivity plots reported in Section 3.2.1 only show results for a 30 cm reflector and an average sensitivity over the entire design. In order to assess the impact of reflector thicknesses, simulations with reflector thicknesses of 0.1, 3.0, 5.0, 15.0, and 30 cm were run. Figures 9-11, show how the sensitivities to ^{63}Cu elastic, ^{63}Cu (n, γ), and ^{235}U total nu change as the Cu reflector thickness increases.

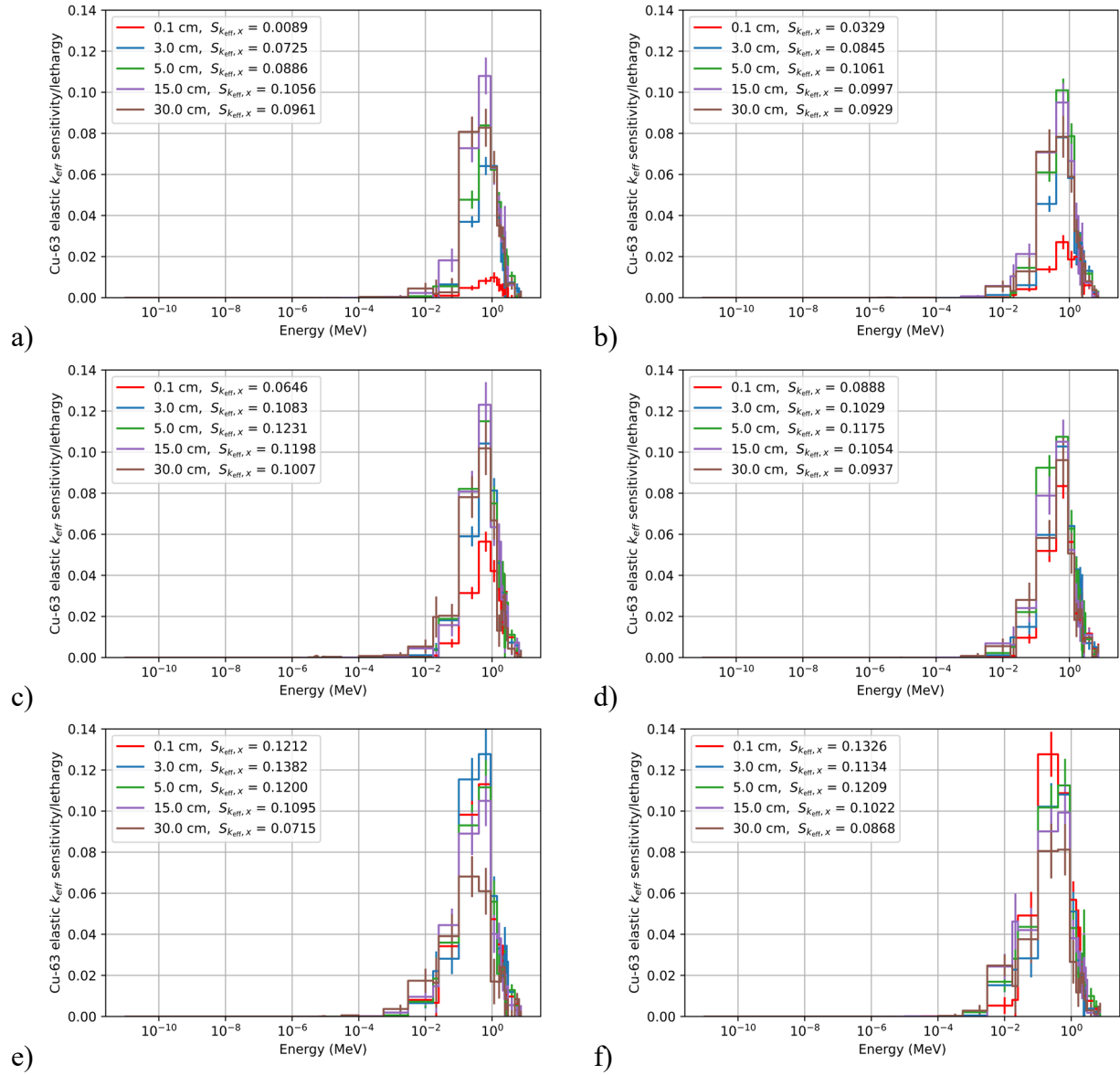


Figure 9: Compares ^{63}Cu elastic scattering sensitivities between various reflector thicknesses for Cu interstitial thicknesses of a) 0.1 cm, b) 0.3 cm, c) 0.7 cm, d) 1.0 cm, e) 3.0 cm, and f) 6.0 cm. All configurations only include 5 units.

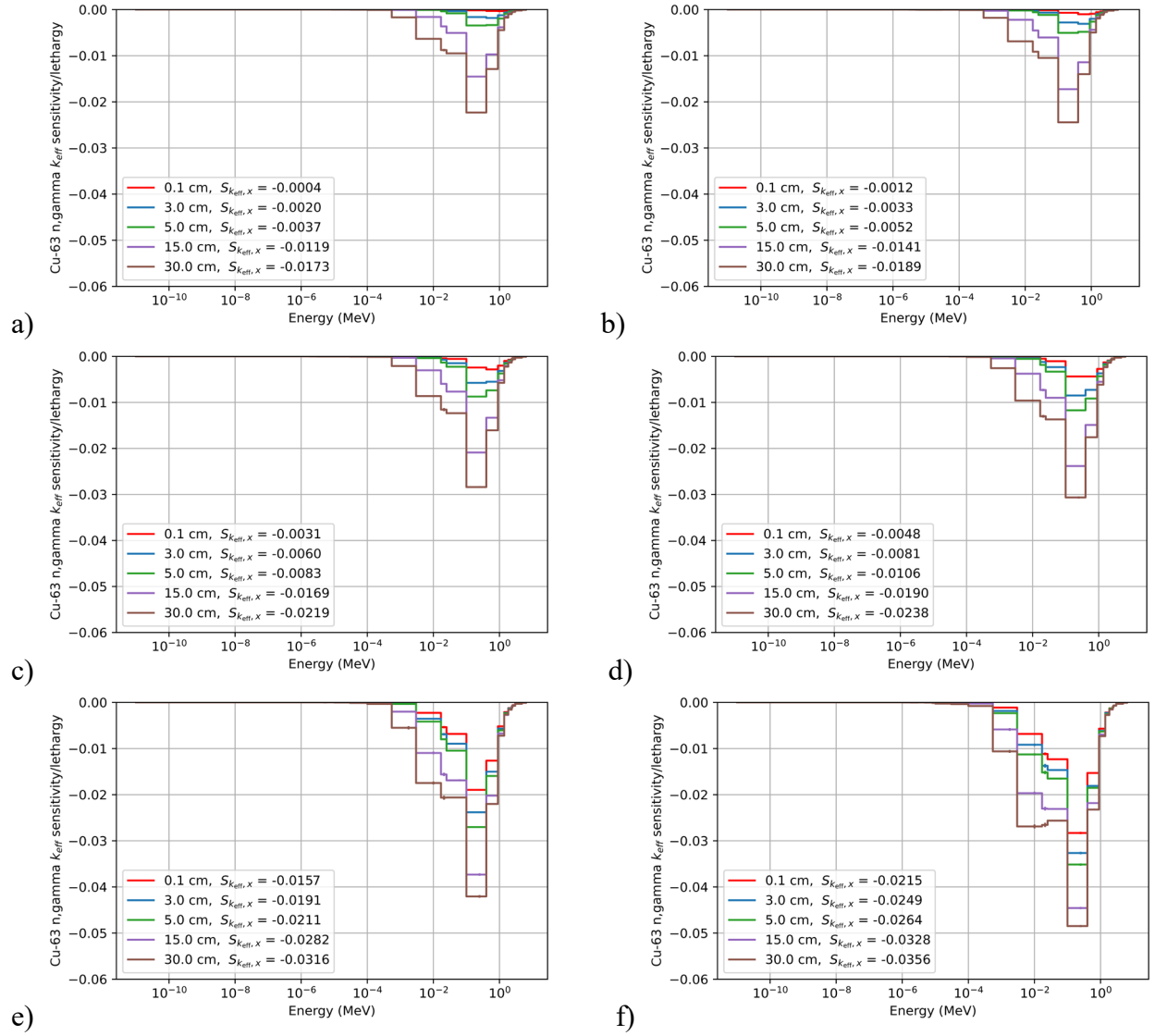


Figure 10: Compares ^{63}Cu (n, γ) sensitivities between various reflector thicknesses for Cu interstitial thicknesses of a) 0.1 cm, b) 0.3 cm, c) 0.7 cm, d) 1.0 cm, e) 3.0 cm, and f) 6.0 cm. All configurations only include 5 units.

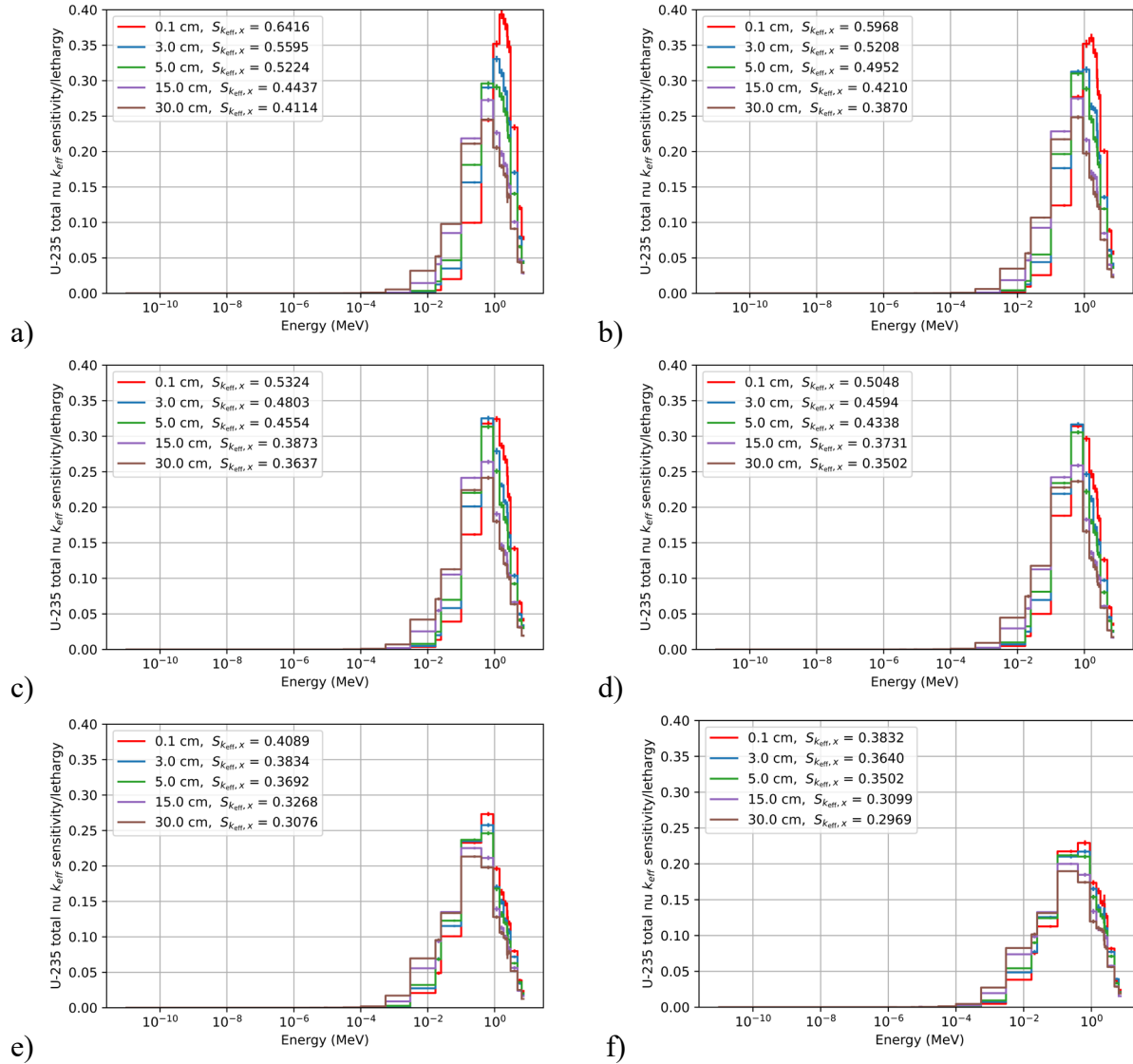


Figure 11: Compares ^{235}U total nu sensitivities between various reflector thicknesses for Cu interstitial thicknesses of a) 0.1 cm, b) 0.3 cm, c) 0.7 cm, d) 1.0 cm, e) 3.0 cm, and f) 6.0 cm. All configurations only include 5 units.

Varying the reflector thickness did help alter the scattering sensitivities, but using only Cu and HEU does not provide the appropriate scattering to reach intermediate energies. Therefore, another material within the core is required.

3.2.3. Critical Configuration

While the base geometry does not achieve intermediate energies, it may be useful in an experiment series as a reference point. Therefore, multiple Cu interstitial thicknesses were evaluated to see how many units it would take to reach a critical configuration. The Cu interstitial thicknesses included in this evaluation are 0.5, 0.6, 0.7, 0.8, 0.9, 1.0, and 2.0 cm. After

adding 12 units, all the Cu thicknesses were able to reach a $k_{\text{eff}} > 1.02$, except 2.0 cm. Figures 12 - 14 compare the sensitivities between 5 units and 12 units

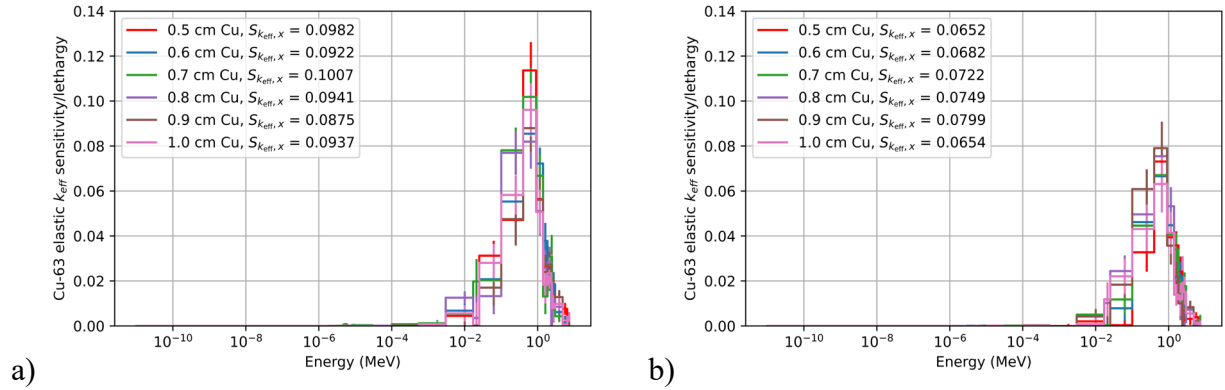


Figure 12: (a) ^{63}Cu elastic scattering sensitivity plotted as a function of energy for Cu interstitial thicknesses of 0.5, 0.6, 0.7, 0.8, 0.9, and 1.0cm in a 5 unit configuration. (b) ^{63}Cu elastic scattering sensitivity plotted as a function of energy for Cu interstitial thicknesses of 0.5, 0.6, 0.7, 0.8, 0.9, and 1.0cm in a 12 unit configuration.

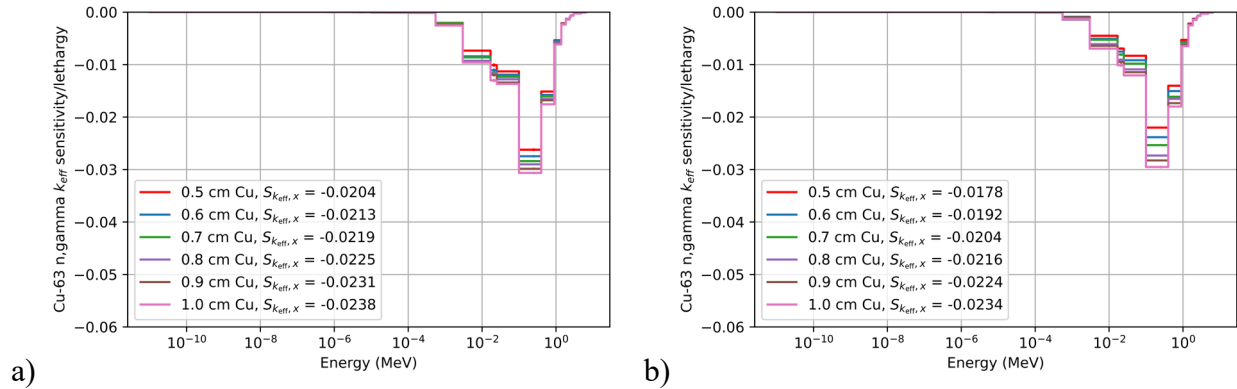


Figure 13: (a) ^{63}Cu (n, γ) sensitivity plotted as a function of energy for Cu interstitial thicknesses of 0.5, 0.6, 0.7, 0.8, 0.9, and 1.0cm in a 5 unit configuration. (b) ^{63}Cu (n, γ) sensitivity plotted as a function of energy for Cu interstitial thicknesses of 0.5, 0.6, 0.7, 0.8, 0.9, and 1.0cm in a 12 unit configuration.

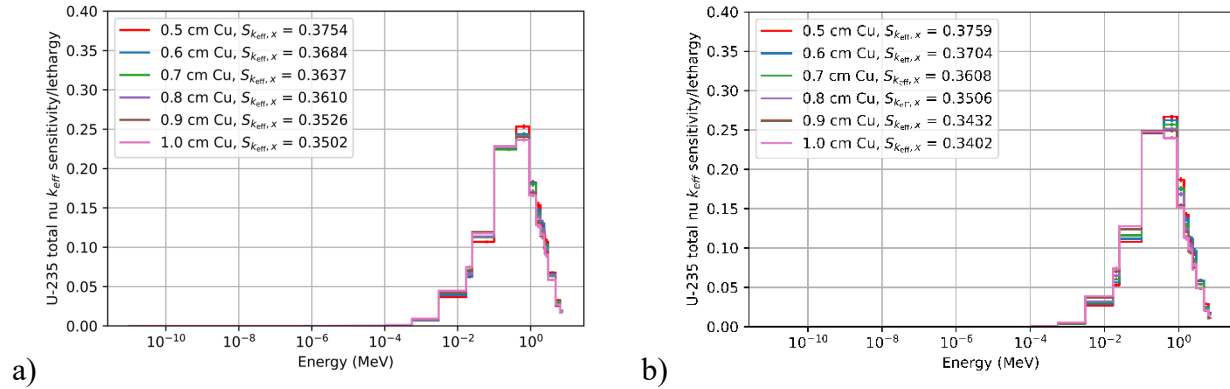


Figure 14: (a) ^{235}U total nu sensitivity plotted as a function of energy for Cu interstitial thicknesses of 0.5, 0.6, 0.7, 0.8, 0.9, and 1. cm in a 5 unit configuration. (b) ^{235}U total nu sensitivity plotted as a function of energy for Cu interstitial thicknesses of 0.5, 0.6, 0.7, 0.8, 0.9, and 1.0cm in a 12 unit configuration.

Based off initial sensitivities and the ability for the system to be critical with ≤ 12 units, 6 Cu interstitial thicknesses are feasible (0.5, 0.6, 0.7, 0.8, 0.9, and 1.0 cm). 12 units was used as the maximum number of units allowed because there is a height limit for experiments on Comet. A more detailed analysis on the each configuration height will be performed in CED-2. Table 4 summarizes the H/D and percent of fissions that are thermal, intermediate, and fast for each of the feasible Cu interstitial thicknesses in the base configuration. The major reactions in these configurations are: ^{235}U total nu, ^{235}U fission, ^{63}Cu elastic, ^{65}Cu elastic, ^{63}Cu (n, γ), ^{235}U (n, γ), ^{63}Cu inelastic, ^{65}Cu (n, γ), ^{235}U inelastic, and ^{65}Cu inelastic. There are some slight differences in the order, but the top three reactions remain the same. For a Cu thickness of 0.6cm, the ^{63}Cu (n, p) reaction does replace ^{235}U inelastic.

Table 4: H/D ratios of the core for feasible Cu interstitial thicknesses for the base configuration. This is the H/D for 12 units and a diameter of 53.34cm. This table also includes the MCNP calculated % thermal, intermediate, and fast fissions.

Cu Interstitial Thickness [cm]	k_{eff}	H/D	% Thermal	% Inter.	% Fast
0.5	1.11404	0.2924	0	23.91	76.09
0.6	1.09340	0.3374	0	25.15	74.85
0.7	1.0742	0.3824	0	26.40	73.60
0.8	1.05548	0.4274	0	27.51	72.49
0.9	1.03797	0.4724	0	28.66	71.34
1.0	1.02147	0.5174	0	29.69	70.31

3.3. Base+

As the results of base show, it is not possible to reach intermediate energies with Cu as the only interstitial material. Therefore, another material needs to be added to the core to soften the neutron spectrum. Adding another material to the design can create complications when trying to isolate specific reactions, so only materials with well-known nuclear data were investigated. Furthermore, the additional interstitial materials are required to have a low neutron capture cross-section. The materials considered are shown in Table 5. More discussion on the results of these materials is included in Sections 3.3.1-3.3.4.

Table 5: Materials considered as a second interstitial material in base+.

Material Name	Chemical Formula	Density [g/cm ³]
Polyethylene ^{14,15}	C ₂ H ₄	0.93
Alumina ¹⁶	Al ₂ O ₃	3.90
Silicon Carbide ¹⁷	SiC	3.16
Silicon Dioxide ¹⁸	SiO ₂	2.65

Simulations that varied both the Cu interstitial thickness and the second interstitial material were performed. The thicknesses of each interstitial material was varied from 0.1 to 6.0 cm, with 15 different thicknesses included in that range. Given the significant number of simulations for each new interstitial material tested, only the sensitivity results from the most promising subsets are included in this report. A sample input for base+ can be found in Appendix E.

3.3.1. Polyethylene

Polyethylene is a well-known material that is commonly used to thermalize neutrons. In order to be sensitive in the intermediate energy region, the poly in the core has to be quite thin; otherwise, the thermal peaks get too large and an intermediate system is no longer viable. Based off the ⁶³Cu elastic scattering and the ²³⁵U total nu sensitivities from the initial set of 225 simulations, the ideal

¹⁴ Polyethylene is the only material that uses an S(α , β) card in the CED-1 simulations and the h-poly.40t card was used. This is the latest S(α , β) for ENDF/B-VIII.0 that was released in July 2020 for room temperature.

¹⁵ Density & chemical formula: <https://omnexus.specialchem.com/selection-guide/polyethylene-plastic>. Note, there are a range of densities for polyethylene, so a value that is included in the high-density and low-density ranges was chosen. The material card definition was calculated from the chemical composition.

¹⁶ Density & chemical formula: <https://www.azom.com/properties.aspx?ArticleID=52>. Note there is an acceptable range of densities for alumina 3-3.98 g/cm³, so a value near the theoretical density was chosen. The material card definition was calculated from the chemical composition.

¹⁷ Density & chemical formula: <https://www.americanelements.com/silicon-carbide-409-21-2>. Note there is an acceptable range of densities for SiC 3-3.2 g/cm³, so a value near the theoretical density was chosen. The material card definition was calculated from the chemical composition.

¹⁸ Density & chemical formula: <https://www.azom.com/properties.aspx?ArticleID=1114>. Note there is an acceptable range of densities for SiO₂ 2.17-2.65 g/cm³, so the theoretical density was chosen, since we are looking at a solid sheet of SiO₂, rather than amorphous SiO₂. The material card definition was calculated from the chemical composition.

thickness for the poly interstitial is 0.3cm. Figure 15 shows how k_{eff} changes as the Cu interstitial thickness is increased. Whether the system is critical with five units is not of concern when initially deciding on a configuration because more units can be added, but will be assessed at the end of each section before making a final determination. Figures 16 – 18 show the ^{63}Cu elastic scattering, ^{63}Cu (n, γ), and ^{235}U total nu sensitivities for all the configurations with 0.3cm thick poly interstitial.

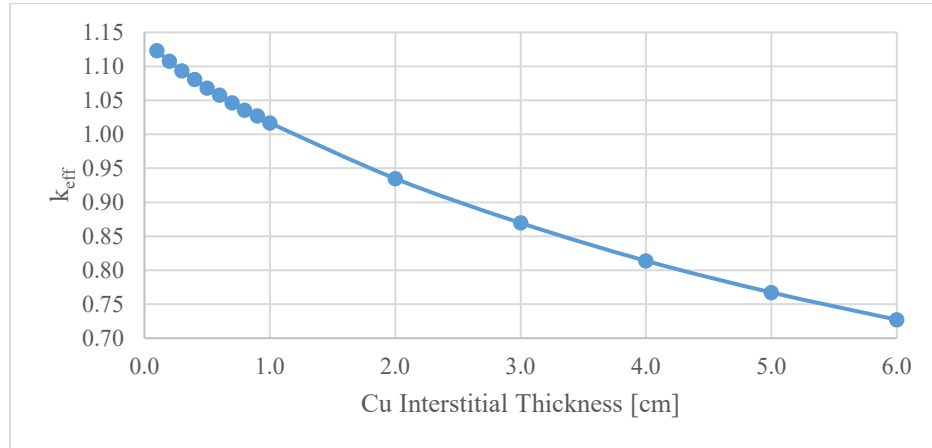
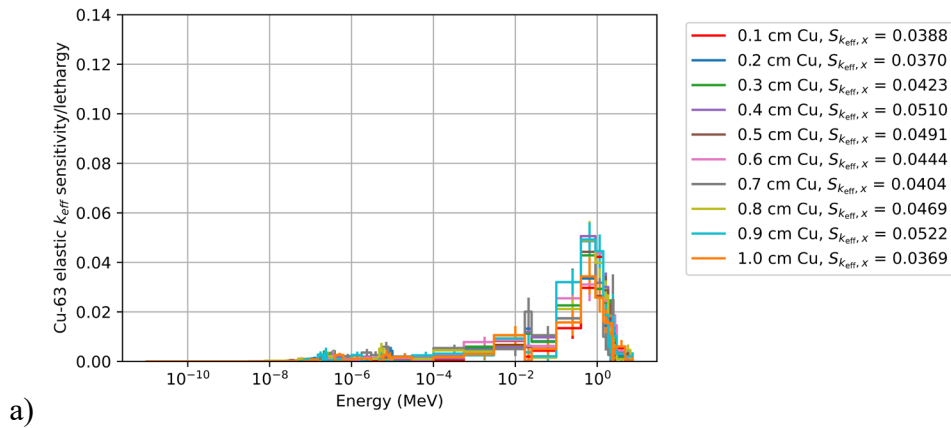


Figure 15: k_{eff} vs. Cu interstitial thickness for an interstitial polyethylene thickness of 0.3cm. Configuration only includes 5 units and a 30cm Cu reflector.



a)

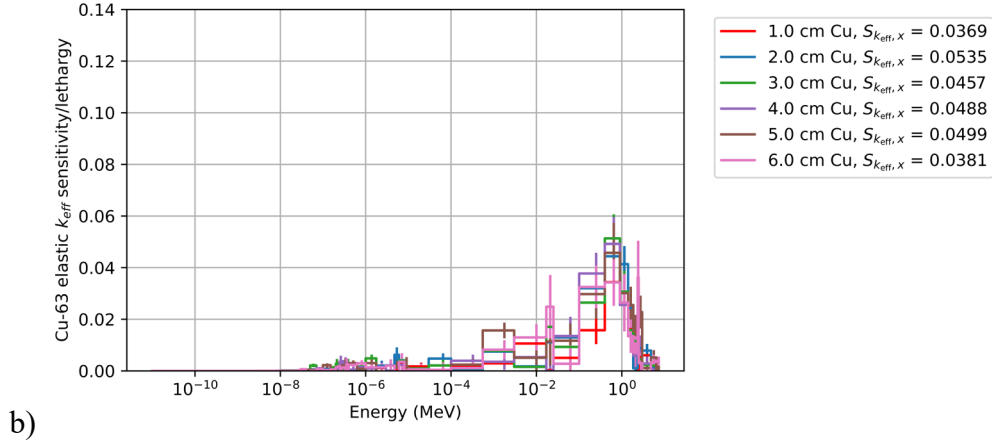


Figure 12: ^{63}Cu elastic scattering sensitivities for configurations with a 0.3cm poly interstitial thickness and varying Cu interstitial thicknesses: a) 0.1cm – 1.0cm and b) 1.0cm – 6.0cm. Configurations only include 5 units and a 30cm Cu reflector.

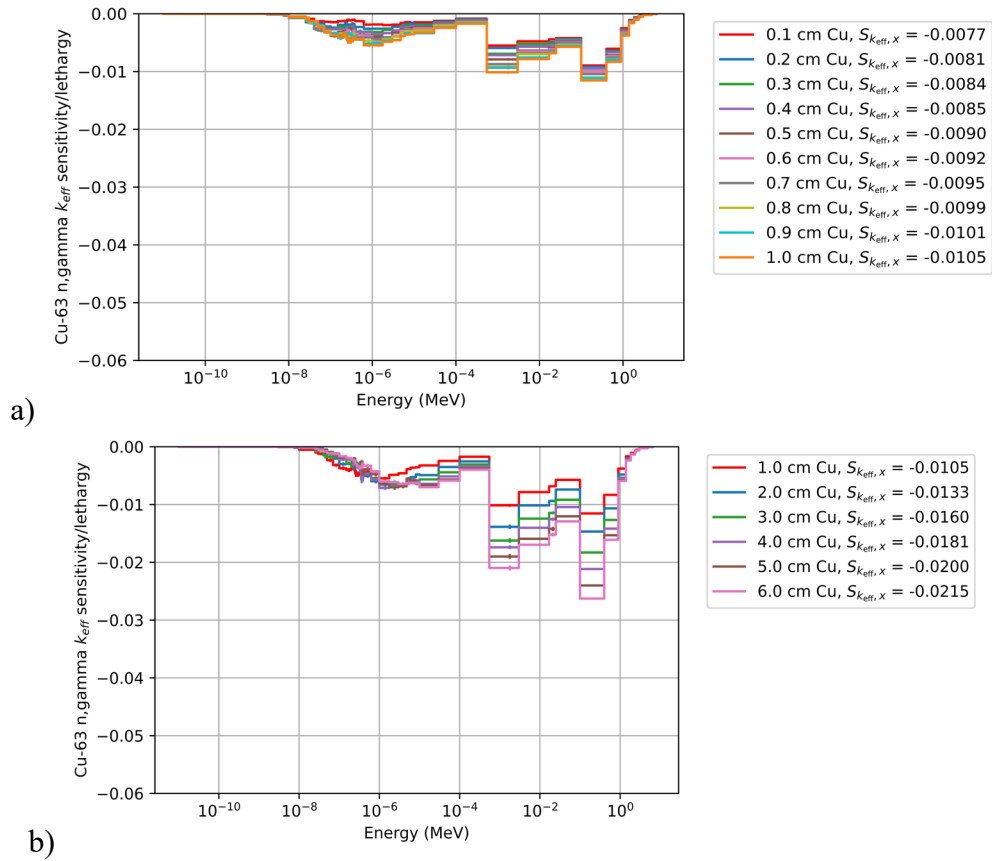


Figure 13: ^{63}Cu (n, γ) sensitivities for configurations with a 0.3cm poly interstitial thickness and varying Cu interstitial thicknesses: a) 0.1cm – 1.0cm and b) 1.0cm – 6.0cm. Configurations only include 5 units and a 30cm Cu reflector.

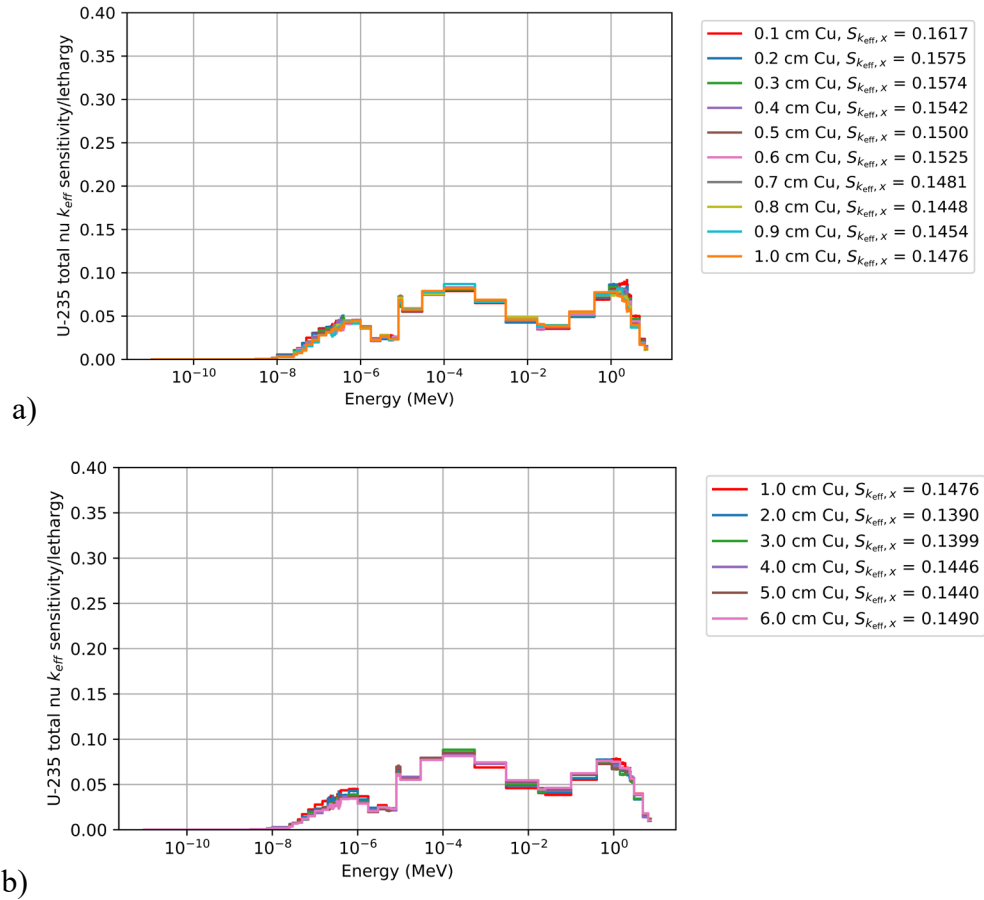


Figure 14: ^{235}U total nu sensitivities for configurations with a 0.3cm poly interstitial thickness and varying Cu interstitial thicknesses: a) 0.1cm – 1.0cm and b) 1.0cm – 6.0cm. Configurations only include 5 units and a 30cm Cu reflector.

Based off the sensitivities above, a Cu interstitial thickness of 1.0cm seemed promising and additional studies were performed, to see if their results were useful. The sensitivity of angular distribution within Cu elastic scattering is of interest to the nuclear data community as well as the P1-energy sensitivities. However, longer simulations are required to achieve appropriate statistics to make plots of those sensitivities useful. Varying the reflector thickness showed potential in the base design, so a similar analysis was included for base+ with polyethylene. Figure 19 shows the change in ^{63}Cu elastic scattering, ^{63}Cu (n, γ), and ^{235}U total nu as the Cu reflector thickness is varied. Figure 20 shows the elastic law sensitivities for cosine scattering angle and for P1 Legendre Moment over energy. The additional analysis shown here displays the effects of varying reflector thickness, but will not be repeated for other interstitial materials in CED-1. Instead, this analysis will be performed in CED-2 along with optimizing the reflector thicknesses and further down selecting the experiment configurations.

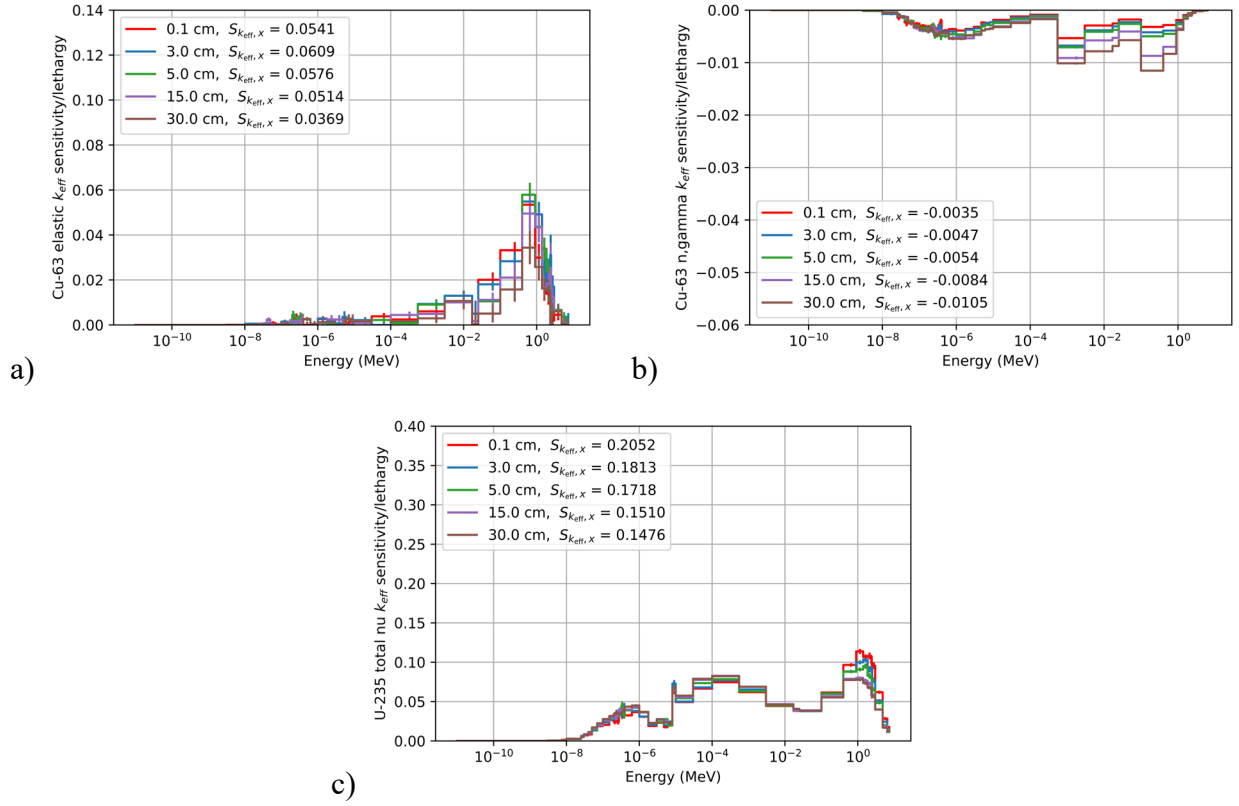


Figure 19: Change in sensitivities as the Cu reflector is varied (0.1, 3.0, 5.0, 15.0, 30.0 cm) for a 5 unit configuration with a 1.0cm Cu interstitial thickness and a 0.3cm polyethylene thickness. Plot a) ^{63}Cu elastic scattering, b) ^{63}Cu (n,γ), and c) ^{235}U total nu.

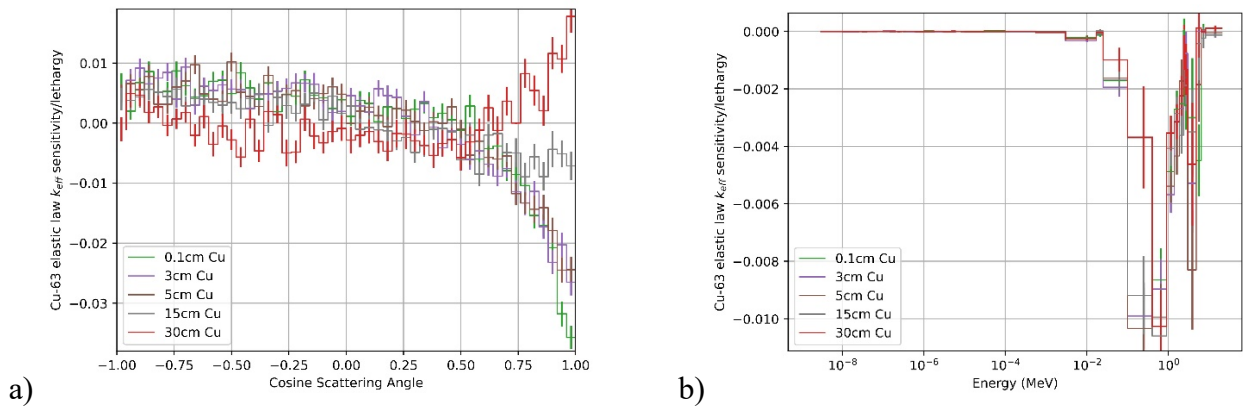


Figure 20: Elastic law sensitivities for varying reflector thicknesses a) cosine scattering angle and b) P1 Legendre Moment over energy. This 5 unit configuration has a 0.3cm poly interstitial thickness and a 1.0cm Cu interstitial thickness.

Based off the sensitivities above, base+ with polyethylene meets the design criteria better than base since intermediate energies can be achieved. Furthermore, varying the reflector thickness allows for changes in the sensitivity profiles with the same core configuration. The results from the elastic law sensitivities for cosine scattering angle also show a change with varying reflector thickness. This makes varying the reflector thickness a useful parameter for the experiment design and will be further investigated in CED-2.

To improve the understanding of the design, additional simulations of the 1.0cm Cu interstitial and 0.3cm poly interstitial configuration were run to look into the effect of the core. Based off the HEU fuel available in the NCERC inventory, the core can be 53.34cm (21in) in diameter (which was modeled in all the previous simulations) or 38.10cm (15in) in diameter. Figure 21 compares the sensitivities between a configuration with a 53.34cm core and a 38.10cm core. It is also important to know what component is contributing the most to the total sensitivity.

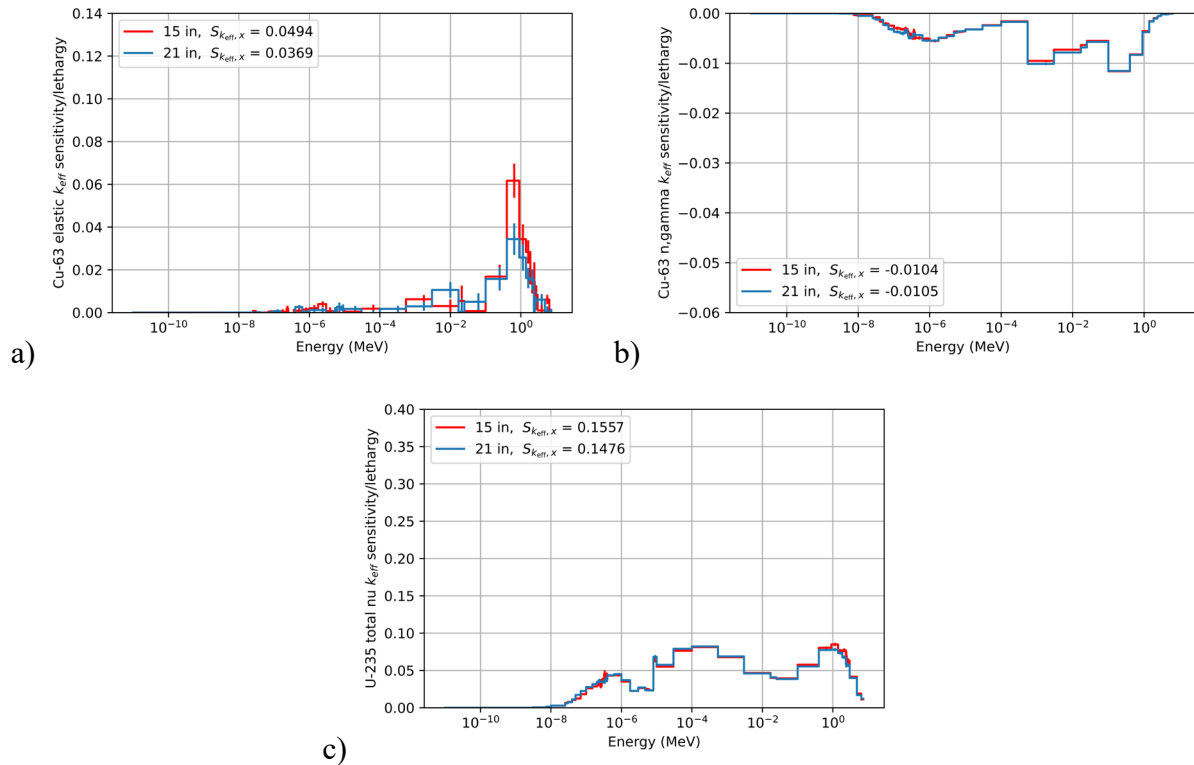


Figure 21: Comparing sensitivities between a 38.10cm (15in) core (red) and a 53.34cm (21in) core (blue). Configurations only include 5 units and a 30cm Cu reflector. Plot a) ^{63}Cu elastic scattering, b) ^{63}Cu (n, γ), and c) ^{235}U total nu.

Based off the results in Figure 21, there is an increase in the ^{63}Cu elastic scattering sensitivity for the smaller core diameter without impacting other reactions of interest. While the analysis of the core diameter showed a higher ^{63}Cu elastic sensitivity for the 38.10cm diameter, all remaining simulations use a 53.34cm core. Further investigation into using a 38.10cm core will be performed in CED-2.

Additional units were added to the poly configuration to see if the 1.0cm Cu and 0.3cm poly configuration can go critical. This configuration requires 9 units to reach a $k_{\text{eff}} = 1.04564$, with an H/D of 0.6524 (%Thermal = 18.54, %Intermediate = 58.90, and %Fast = 22.56). Figure 22 compares the ^{63}Cu elastic scattering, $^{63}\text{Cu}(n,\gamma)$, and ^{235}U total nu sensitivities between a configuration with a Cu interstitial thickness of 1.0cm and a poly interstitial thickness of 0.3cm for 5 units and 9 units. The major reactions in this configuration is: ^{235}U total nu, ^{235}U fission, ^1H elastic, $^{235}\text{U}(n,\gamma)$, ^{63}Cu elastic, $^{63}\text{Cu}(n,\gamma)$, ^{12}C elastic, ^{63}Cu inelastic, ^{65}Cu elastic, and $^1\text{H}(n,\gamma)$.

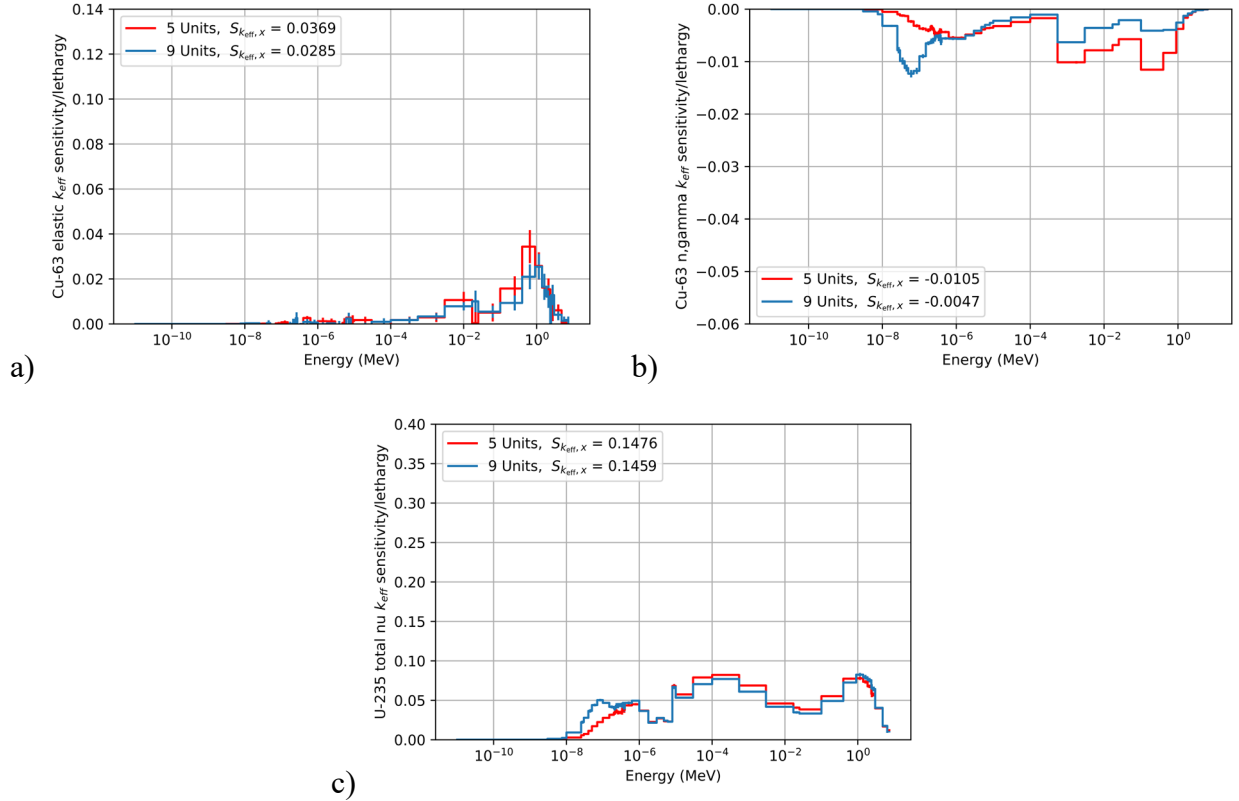


Figure 22: (a) ^{63}Cu elastic scattering, (b) $^{63}\text{Cu}(n,\gamma)$, and (c) ^{235}U total nu sensitivity plotted as a function of energy for Cu interstitial thickness of 1.0cm, polyethylene interstitial thickness of 0.3cm, and Cu reflector thickness of 30.0cm in 5 unit (red) and 9 unit (blue) configurations.

While the base+ configuration with polyethylene does help achieve a more intermediate system than base, thermal peaks (small or large) exist in each configuration. This provides an additional challenge when trying to isolate reactions in specific energy regions. Therefore, additional interstitial materials that are not as effective at thermalizing neutrons were considered.

3.3.2. Alumina

A similar methodology described in Section 3.3.1 was used for the remaining interstitial materials investigated as part of base+. Alumina (Al_2O_3) is a well-known material that has a higher density

than polyethylene. In order to be sensitive in the intermediate energy region, thicker alumina layers are required, which has a negative impact on k_{eff} . However, the Cu interstitial thickness has a greater impact on k_{eff} than the alumina thickness. Therefore, alumina thicknesses between 0.9 and 2.0cm and Cu thicknesses between 0.3 and 0.5cm were investigated. The resulting k_{eff} and sensitivities are reported in Appendix A.

12 units were added to configurations with 0.9 – 2.0cm alumina and 0.3 – 0.5cm of Cu to see if that was enough to have a system with a $k_{\text{eff}} \geq 1.02$, while still achieving an intermediate system. The configurations that best met that criteria are shown in Figure 23 - 25, where the sensitivities between a 5 unit configuration and a 12 unit configuration are compared. Table 6 shows the H/D and percent of fissions that are thermal, intermediate, and fast for all configurations run with 12 units. The major reactions in these configurations are: ^{235}U total nu, ^{235}U fission, ^{16}O elastic, ^{235}U (n, γ), ^{63}Cu elastic, ^{63}Cu (n, γ), ^{27}Al elastic, ^{65}Cu elastic, ^{65}Cu (n, γ), ^{63}Cu inelastic. ^{63}Cu elastic becomes the third highest sensitivity for configurations with 1.0cm alumina.

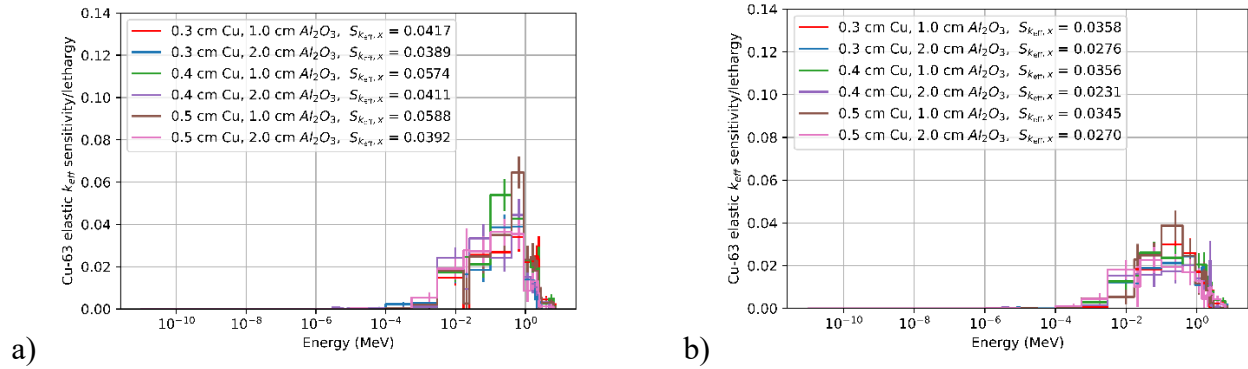


Figure 23: (a) ^{63}Cu elastic scattering sensitivity plotted as a function of energy for Cu interstitial thicknesses of 0.3 – 0.5cm and alumina thicknesses of 1.0 – 2.0cm in a 5 unit configuration. (b) ^{63}Cu elastic scattering sensitivity plotted as a function of energy Cu interstitial thicknesses of 0.3 – 0.5cm and alumina thicknesses of 1.0 – 2.0cm in a 12 unit configuration.

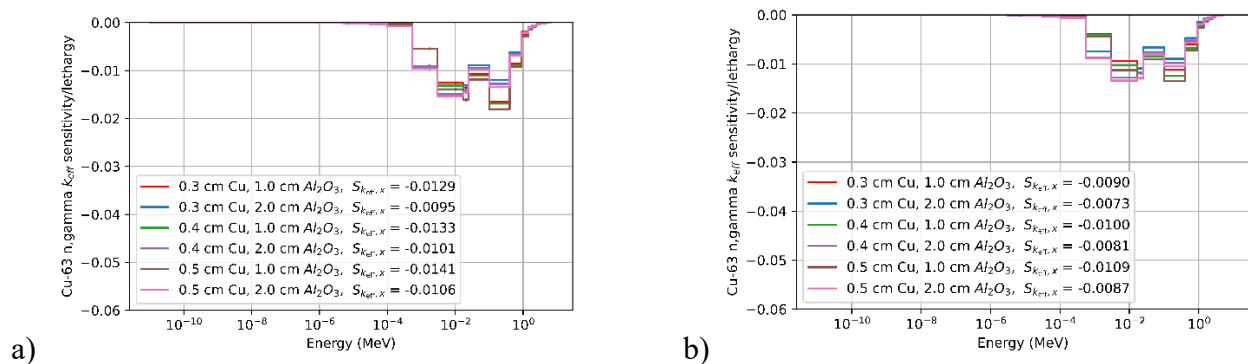


Figure 24: (a) ^{63}Cu (n, γ) sensitivity plotted as a function of energy for Cu interstitial thicknesses of 0.3 – 0.5cm and alumina thicknesses of 1.0 – 2.0cm in a 5 unit configuration. (b) ^{63}Cu (n, γ) sensitivity plotted as a function of energy Cu interstitial thicknesses of 0.3 – 0.5cm and alumina thicknesses of 1.0 – 2.0cm in a 12 unit configuration.

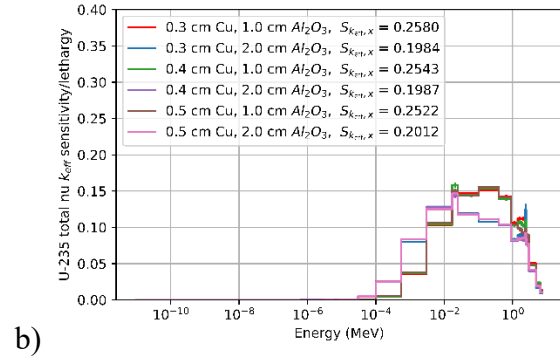
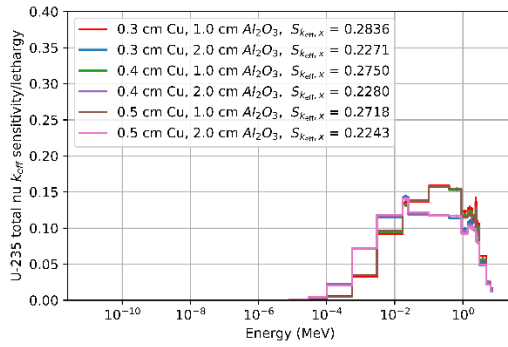


Figure 25: ^{235}U total nu sensitivity plotted as a function of energy for Cu interstitial thicknesses of 0.3 – 0.5cm and alumina thicknesses of 1.0 – 2.0cm in a 5 unit configuration. (b) ^{235}U total nu sensitivity plotted as a function of energy Cu interstitial thicknesses of 0.3 – 0.5cm and alumina thicknesses of 1.0 – 2.0cm in a 12 unit configuration.

Table 6: H/D ratios of the core for feasible base+ alumina configuration. This is the H/D for 12 units and a diameter of 53.34cm. This table also includes the MCNP calculated % thermal, intermediate, and fast fissions.

Cu Interstitial Thickness [cm]	Alumina Interstitial Thickness [cm]	k_{eff}	H/D	% Thermal	% Inter.	% Fast
0.3	0.9	1.10914	0.6074	0	50.83	49.17
	1.0	1.10303	0.6524	0	52.70	47.30
	2.0	1.05405	1.1023	0	64.62	35.38
0.4	0.9	1.09193	0.6524	0	51.48	48.52
	1.0	1.08710	0.6973	0	53.28	46.72
	2.0	1.03810	1.1473	0	64.79	35.21
0.5	0.9	1.07512	0.6973	0	52.02	47.98
	1.0	1.06984	0.7423	0	53.79	46.21
	2.0	1.02332	1.1923	0	64.92	35.08

The base+ configuration with 1.0 – 2.0cm alumina and 0.3 – 0.5cm of Cu is a significant improvement over the base+ configuration with polyethylene, since there are not thermal peaks in the sensitivity profiles. Those configurations also meet the design criteria described in Section 1.

3.3.3. Silicon Carbide

Silicon Carbide (SiC) is a well-known material that has a higher density than polyethylene, but slightly lower than alumina. In order to be sensitive in the intermediate energy region, thicker SiC layers are required, which has a negative impact on k_{eff} . However, the Cu interstitial

thickness has a greater impact on k_{eff} than the SiC thickness. Therefore, SiC thicknesses between 0.9 and 2.0cm and Cu thicknesses between 0.3 and 0.5cm were investigated. The resulting k_{eff} and sensitivities are reported in Appendix B.

12 units were added to configurations with 0.9 – 2.0cm SiC and 0.3 – 0.5cm of Cu to see if that was enough to have a system with a $k_{\text{eff}} \geq 1.02$, while still achieving an intermediate system. The configurations that best met that criteria are shown in Figure 26 - 28, where the sensitivities between a 5 unit configuration and a 12 unit configuration are compared. Table 7 shows the H/D and percent of fissions that are thermal, intermediate, and fast for those configurations. The major reactions in these configurations are: ^{235}U total nu, ^{235}U fission, ^{63}Cu elastic, ^{235}U (n, γ), ^{12}C elastic, ^{65}Cu elastic, ^{63}Cu (n, γ), ^{28}Si elastic, ^{63}Cu inelastic, and ^{65}Cu (n, γ). The ^{63}Cu elastic is the third highest sensitivity in all configurations except SiC = 2.0cm and Cu = 0.3 or 0.5cm. In those configurations, ^{12}C elastic is the third highest sensitivity and ^{63}Cu elastic is fourth.

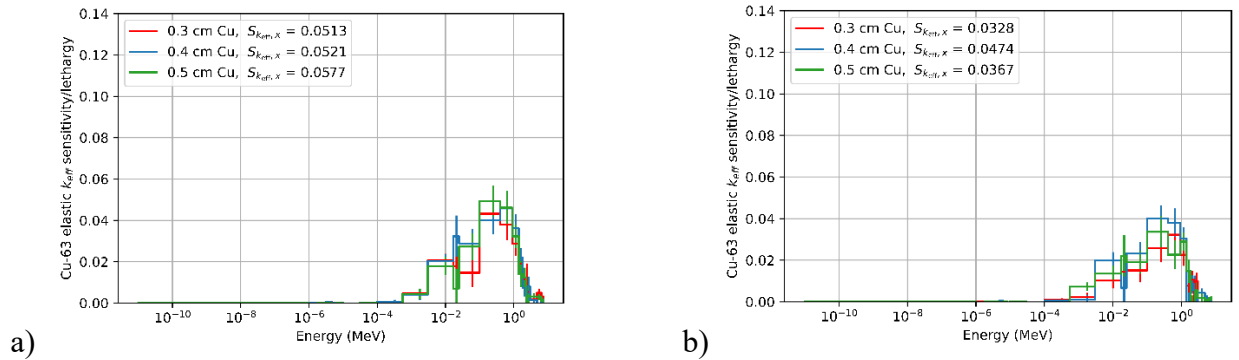


Figure 26: (a) ^{63}Cu elastic scattering sensitivity plotted as a function of energy for Cu interstitial thicknesses of 0.3 – 0.5cm and SiC thicknesses of 2.0cm in a 5 unit configuration. (b) ^{63}Cu elastic scattering sensitivity plotted as a function of energy Cu interstitial thicknesses of 0.3 – 0.5cm and SiC thicknesses of 2.0cm in a 12 unit configuration.

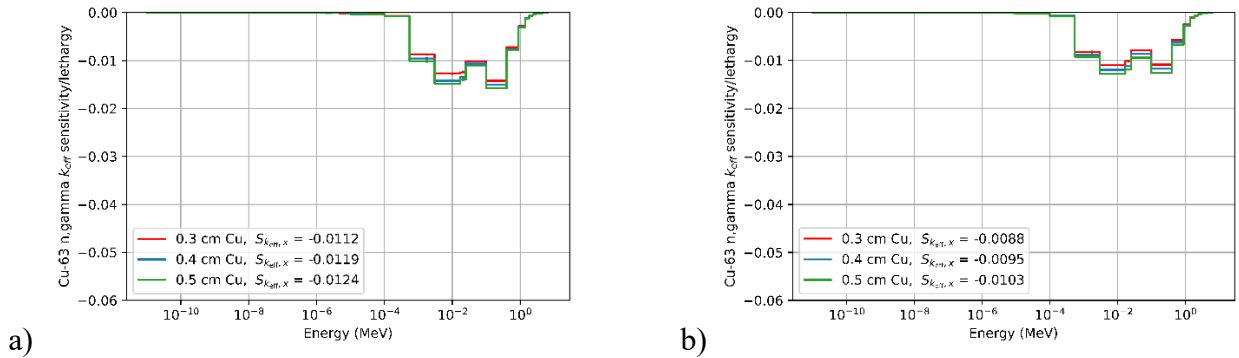


Figure 27: ^{63}Cu (n, γ) sensitivity plotted as a function of energy for Cu interstitial thicknesses of 0.3 – 0.5cm and SiC thicknesses of 2.0cm in a 5 unit configuration. (b) ^{63}Cu (n, γ) sensitivity plotted as a function of energy Cu interstitial thicknesses of 0.3 – 0.5cm and SiC thicknesses of 2.0cm in a 12 unit configuration.

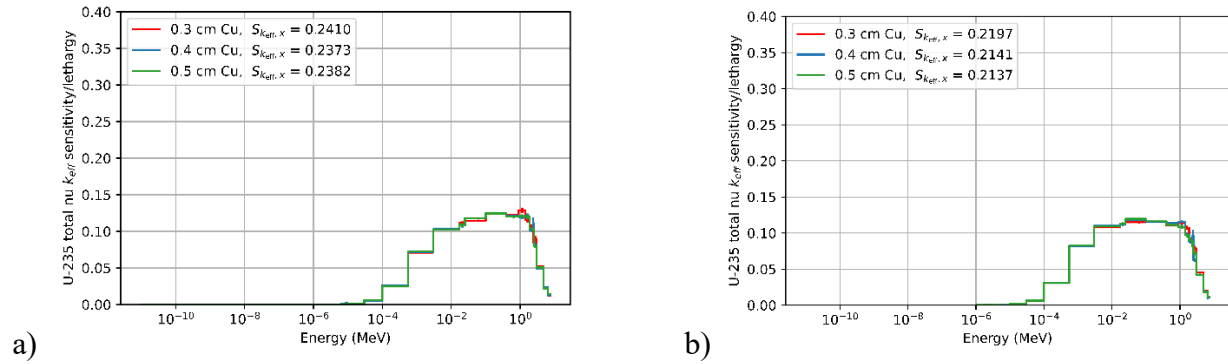


Figure 28: ^{235}U total nu sensitivity plotted as a function of energy for Cu interstitial thicknesses of 0.3 – 0.5cm and SiC thicknesses of 2.0cm in a 5 unit configuration. (b) ^{235}U total nu sensitivity plotted as a function of energy Cu interstitial thicknesses of 0.3 – 0.5cm and SiC thicknesses of 2.0cm in a 12 unit configuration.

Table 7: H/D ratios of the core for feasible base+ SiC configuration. This is the H/D for 12 units and a diameter of 53.34cm. This table also includes the MCNP calculated % thermal, intermediate, and fast fissions.

Cu Interstitial Thickness [cm]	SiC Interstitial Thickness [cm]	k_{eff}	H/D	% Thermal	% Inter.	% Fast
0.3	0.9	1.08192	0.6074	0	47.57	52.43
	1.0	1.07508	0.6524	0	49.32	50.68
	2.0	1.02129	1.1023	0	61.21	38.78
0.4	0.9	1.06629	0.6524	0	48.31	51.69
	1.0	1.05927	0.6973	0	50.07	49.93
	2.0	1.00759	1.1473	0	61.5	38.5
0.5	0.9	1.05067	0.6973	0	49.01	50.99
	1.0	1.04387	0.7423	0	50.69	49.31
	2.0	0.99344	1.1923	0	61.72	38.28

The base+ configuration with 1.0cm SiC and 0.4 or 0.5cm Cu or 2.0cm SiC and 0.3cm of Cu is a significant improvement over the base+ configuration with polyethylene, since there are not thermal peaks in the sensitivity profiles. Those configurations also meet the design criteria described in Section 1.

3.3.4. Silicon Dioxide

Silicon Dioxide (SiO_2) is a well-known material that has a higher density than polyethylene, but slightly lower than SiC. In order to be sensitive in the intermediate energy region, thicker SiO_2 layers are required, which has a negative impact on k_{eff} . However, the Cu interstitial thickness

has a greater impact on k_{eff} than the SiO₂ thickness. Therefore, SiO₂ thicknesses between 0.9 – 2.0cm and Cu thicknesses between 0.3 – 0.5cm were investigated. The resulting k_{eff} and sensitivities are reported in Appendix C.

12 units were added to configurations with 0.9 – 2.0cm SiO₂ and 0.3 – 0.5cm of Cu to see if that was enough to have a system with a $k_{\text{eff}} \geq 1.02$, while still achieving an intermediate system. The configurations that best met that criteria are shown in Figure 29 - 31, where the sensitivities between a 5 unit configuration and a 12 unit configuration are compared, but none of the configurations shown are critical. Table 8 shows the H/D and percent of fissions that are thermal, intermediate, and fast for those configurations. The major reactions in these configurations are: ²³⁵U total nu, ²³⁵U fission, ⁶³Cu elastic, ¹⁶O elastic, ²³⁵U (n, γ), ⁶³Cu (n, γ), ⁶⁵Cu elastic, ²⁸Si elastic, ⁶³Cu inelastic, ⁶⁵Cu (n, γ). The ⁶³Cu elastic reaction is no longer the third highest sensitivity for the Cu = 0.5cm and SiO₂ = 2.0cm configuration.

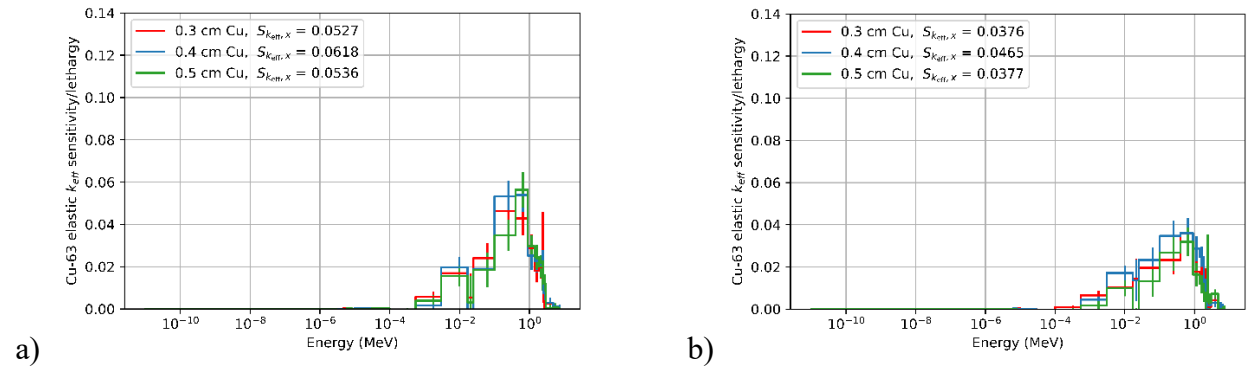


Figure 29: (a) ⁶³Cu elastic scattering sensitivity plotted as a function of energy for Cu interstitial thicknesses of 0.3 – 0.5cm and SiO₂ thicknesses of 2.0cm in a 5 unit configuration. (b) ⁶³Cu elastic scattering sensitivity plotted as a function of energy Cu interstitial thicknesses of 0.3 – 0.5cm and SiO₂ thicknesses of 2.0cm in a 12 unit configuration.

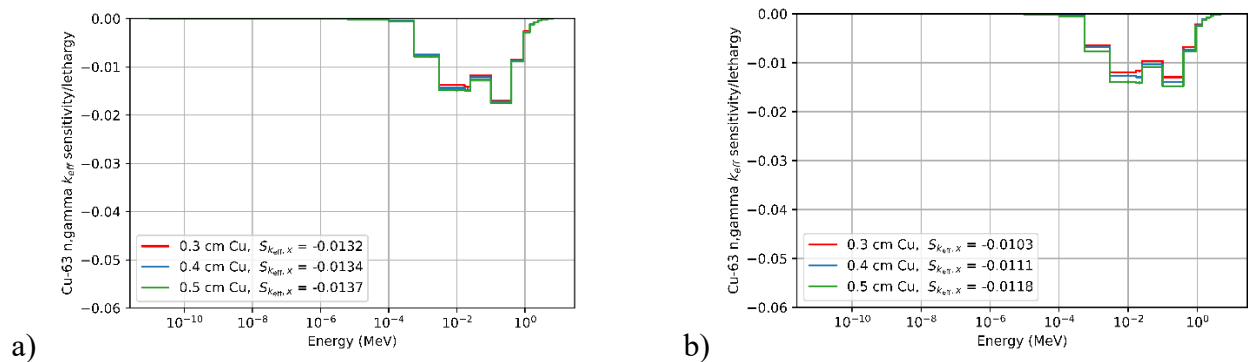


Figure 30: ⁶³Cu (n, γ) sensitivity plotted as a function of energy for Cu interstitial thicknesses of 0.3 – 0.5cm and SiO₂ thicknesses of 2.0cm in a 5 unit configuration. (b) ⁶³Cu (n, γ) sensitivity plotted as a function of energy Cu interstitial thicknesses of 0.3 – 0.5cm and SiO₂ thicknesses of 2.0cm in a 12 unit configuration.

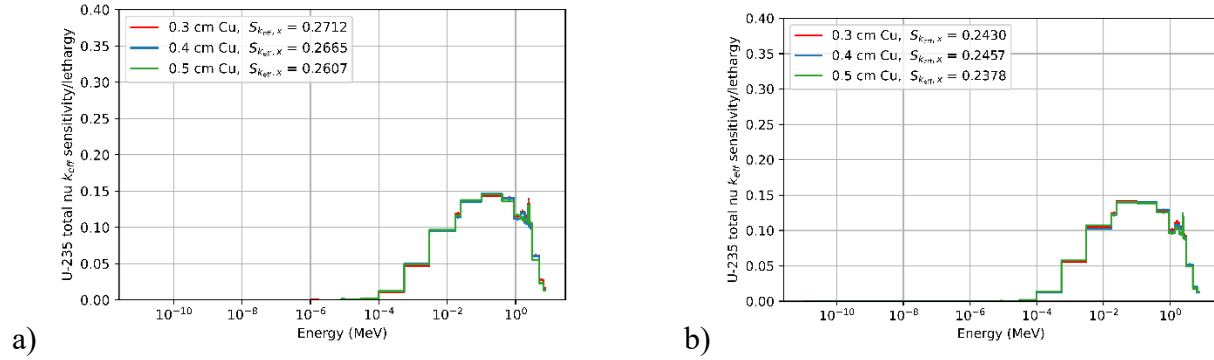


Figure 31: ^{235}U total nu sensitivity plotted as a function of energy for Cu interstitial thicknesses of 0.3 – 0.5cm and SiO_2 thicknesses of 2.0cm in a 5 unit configuration. (b) ^{235}U total nu sensitivity plotted as a function of energy Cu interstitial thicknesses of 0.3 – 0.5cm and SiO_2 thicknesses of 2.0cm in a 12 unit configuration.

Table 8: H/D ratios of the core for feasible base+ SiO_2 configuration. This is the H/D for 12 units and a diameter of 53.34cm. This table also includes the MCNP calculated % thermal, intermediate, and fast fissions.

Cu Interstitial Thickness [cm]	SiO_2 Interstitial Thickness [cm]	k_{eff}	H/D	% Thermal	% Inter.	% Fast
0.3	0.9	1.04954	0.6074	0	42.96	57.04
	1.0	1.03945	0.6524	0	44.61	55.39
	2.0	0.96286	1.1023	0	55.96	44.04
0.4	0.9	1.03462	0.6524	0	43.82	56.18
	1.0	1.02606	0.6973	0	45.46	54.54
	2.0	0.95189	1.1473	0	56.39	43.61
0.5	0.9	1.01986	0.6973	0	44.63	55.37
	1.0	1.01182	0.7423	0	46.22	53.78
	2.0	0.93976	1.1923	0	56.75	43.25

The base+ configuration with 2.0cm SiO_2 and 0.3 – 0.5cm of Cu is a significant improvement over the base+ configuration with polyethylene, since there are not thermal peaks in the sensitivity profiles. However, reaching an intermediate system that is also critical ($k_{\text{eff}} \geq 1.02$) will require further analysis and does not provide any information different than alumina and SiC .

4.0 PRELIMINARY DESIGN DESCRIPTION

Based off the sensitivity analysis, base+ with alumina or silicon carbide as the second interstitial material meets the design criteria listed in Section 1.0. Therefore, it is feasible to create an experiment that 1) maximizes sensitivity to Cu elastic scattering cross sections and angular distributions, 2) targets the intermediate energy region for the neutron flux and Cu elastic scattering sensitivity, and 3) uses materials with well-known nuclear data so Cu sensitivities can be better

isolated. It was also shown that varying the Cu reflector thickness is useful in order to change the sensitivity profile. Sections 4.1 - 4.4 will explain each component of the experiment in further detail.

4.1. Assembly Machine

Given the expected weight of this experiment, Comet will be used for the CERBERUS Experiment. Comet is a vertical lift machine, where the experiment is divided into two parts that are brought together by a moveable platen (see Figure 32). The side and top reflector material will be placed on a stationary platform along with the upper core that is supported by a membrane. Then the lower core and bottom reflector will be placed on the moveable platen, so that it can approach criticality as the moveable platen is raised.



Figure 32: CAD rendering of the Comet vertical assembly machine.

4.2. Fuel

HEU fuel already exists within the NCERC inventory, which can be used in this experiment. The Jemima plates are the ideal candidate, since it is the same fuel that was used in the ZEUS experiment series¹⁹, allowing for a more direct comparison. The Jemima plates are 0.29972cm thick plates that are ~93% enriched with ²³⁵U. The inner Jemima plates have a diameter of 38.10cm and an outer ring can be placed outside the inner plates to increase the diameter to 53.34cm.

¹⁹ HEU-MET-FAST-073, HEU-MET-FAST-072, and HEU-MET-INTER-006

Assessing if only the inner Jemima plates can be used, while reaching a critical configuration, will be discussed in CED-2. The current design will utilize both the inner and outer Jemima plate for a core diameter of 53.34cm.

4.3. Interstitial Materials

The base+ configurations with Alumina and SiC best meet the design criteria described in Section 1. However, the base configuration may also be a useful reference point and using this configuration will be further assessed in CED-2. Table 9 shows the interstitial thicknesses that are best for the base+ configuration.

Table 9: Interstitial material thicknesses for CED-1 experiment configurations.

2 nd Material	2 nd Interstitial Material Thickness [cm]	Cu Interstitial Thickness [cm]	k_{eff}
Alumina	1.0	0.3	1.0303
		0.4	1.08710
		0.5	1.06984
	2.0	0.3	1.05405
		0.4	1.03810
		0.5	1.02332
SiC	1.0	0.4	1.05927
		0.5	1.04387
	2.0	0.3	1.02129

4.4. Reflector Material

Scattering within the Cu interstitial is too small to isolate the ^{63}Cu elastic scattering reaction, so a Cu reflector is necessary to increase the Cu elastic scattering sensitivity. Varying the reflector thicknesses can make a significant difference in the sensitivity profile. Therefore, the CED-1 design will include varying the Cu reflector between 1cm and 30cm and CED-2 will optimize what reflector thicknesses are used.

5.0 CONCLUSIONS

The set of configurations described in Section 4.3 meet the design criteria of 1) maximizing sensitivity to Cu elastic scattering cross sections and angular distributions, 2) targeting the intermediate energy region for the neutron flux and Cu elastic scattering sensitivity, and 3) using materials with well-known nuclear data so Cu sensitivities can be better isolated. The CERBERUS CED-1 configurations are summarized in Table 10.

Table 10: Summary of the CERBERUS CED-1 Design.

Component	Description
Assembly Machine	Comet
Fuel	53.34cm diameter Jemima Plates (HEU)
Interstitial	Table 9 summarizes the Cu and 2 nd interstitial material thicknesses, 53.34cm diameter
Reflector	1.0-30.0cm Cu

APPENDIX A: ALUMINA (Al_2O_3) SENSITIVITY PLOTS

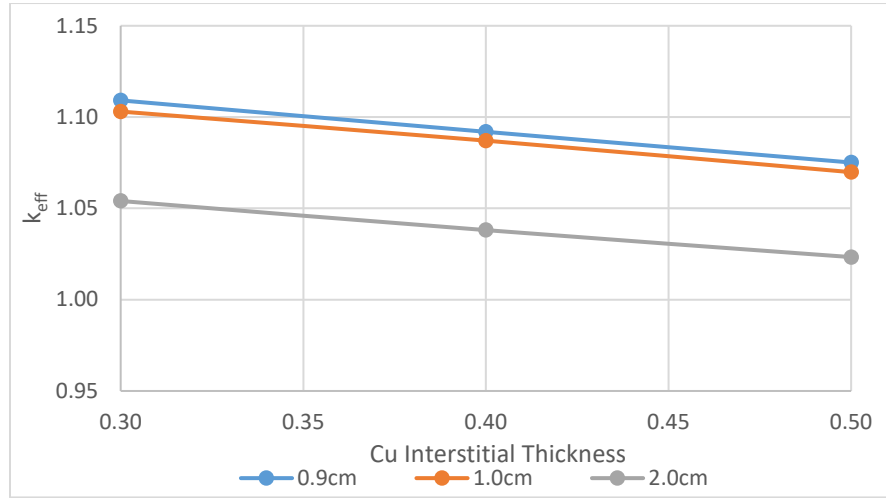


Figure A.1: k_{eff} vs. Cu interstitial thickness for Alumina thickness of 0.9, 1.0, and 2.0cm. All simulations include 5 units and a 30cm Cu reflector

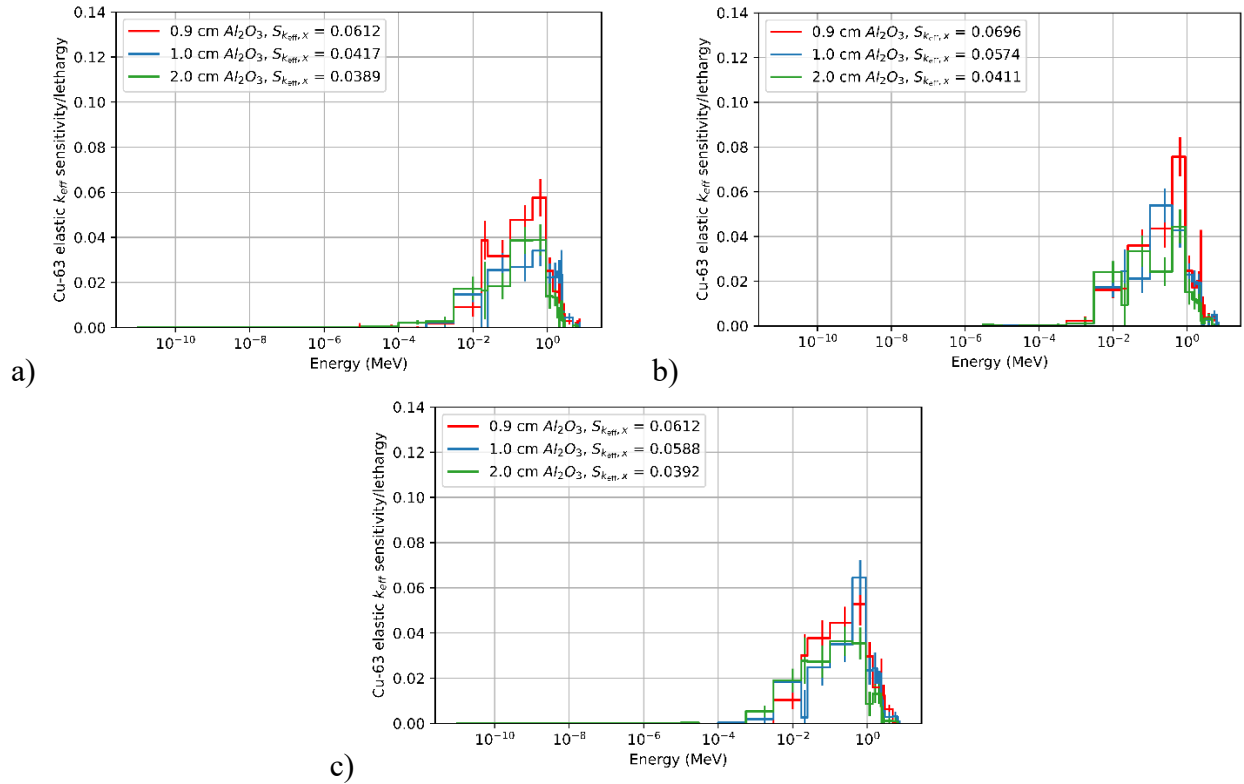


Figure 15: ^{63}Cu elastic scattering sensitivities for configurations with 0.9 – 2.0cm alumina interstitial thickness and Cu interstitial thicknesses: a) 0.3cm, b) 0.4cm, and c) 0.5cm. Configurations only include 5 units and a 30cm Cu reflector.

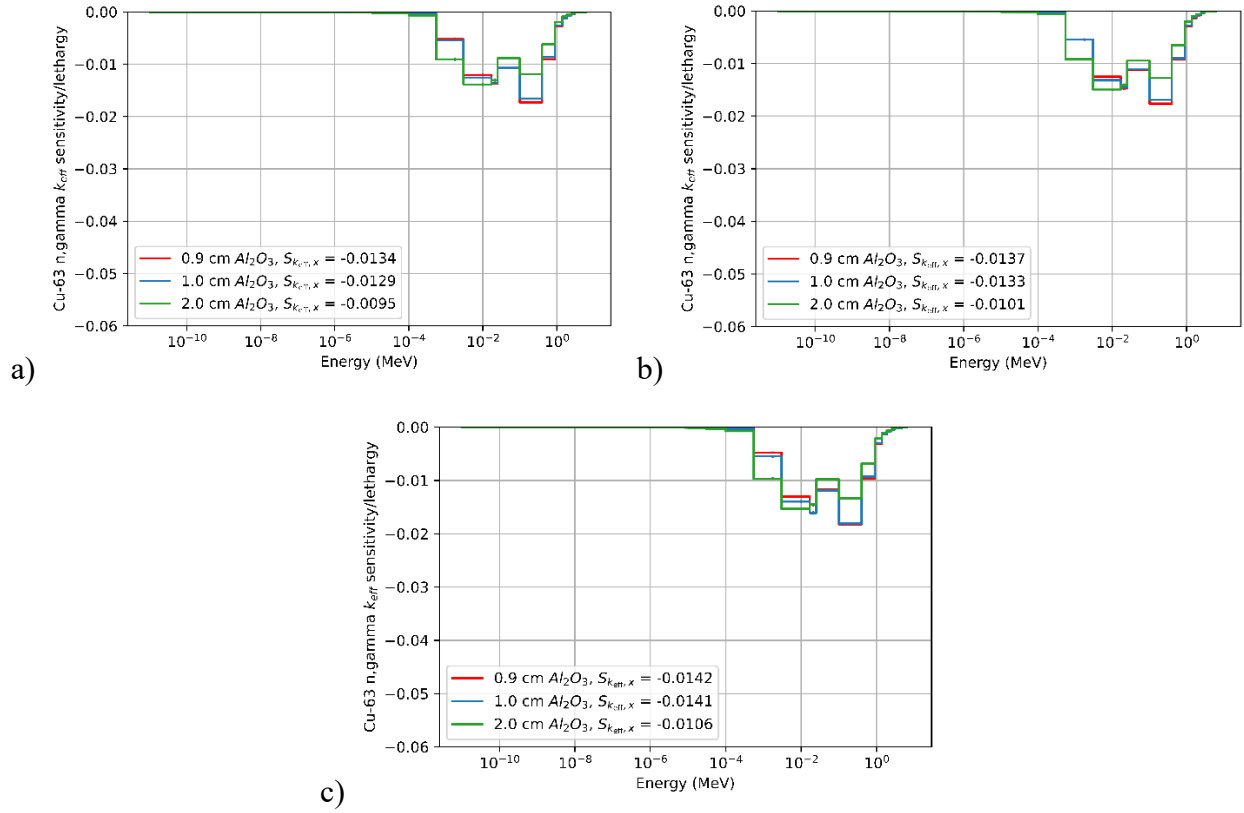


Figure A.3: ^{63}Cu (n, γ) sensitivities for configurations with 0.9 – 2.0cm alumina interstitial thickness and Cu interstitial thicknesses: a) 0.3cm, b) 0.4cm, and c) 0.5cm. Configurations only include five units and a 30cm Cu reflector.

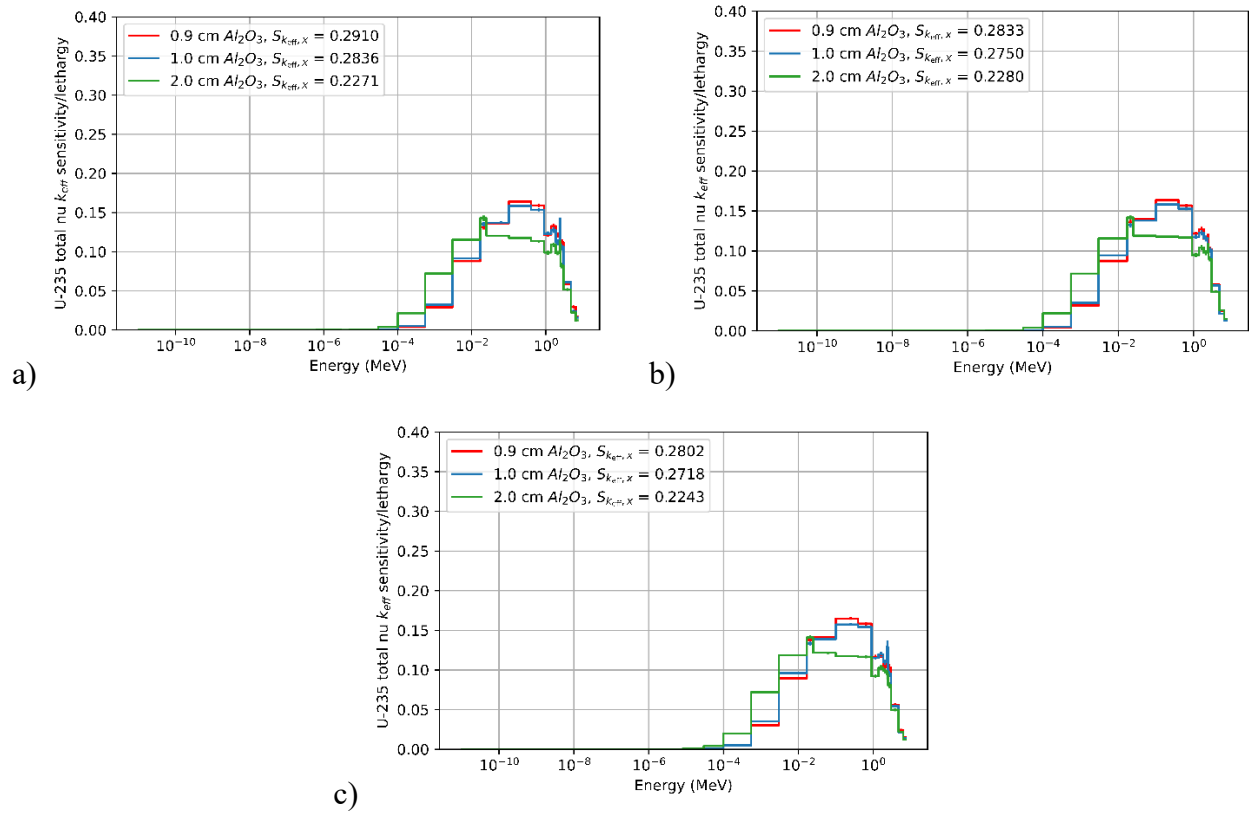


Figure A.4: ^{235}U total nu sensitivities for configurations with 0.9 – 2.0cm alumina interstitial thickness and Cu interstitial thicknesses: a) 0.3cm, b) 0.4cm, and c) 0.5cm. Configurations only include five units and a 30cm Cu reflector.

APPENDIX B: SILICON CARBIDE (SiC) SENSITIVITY PLOTS

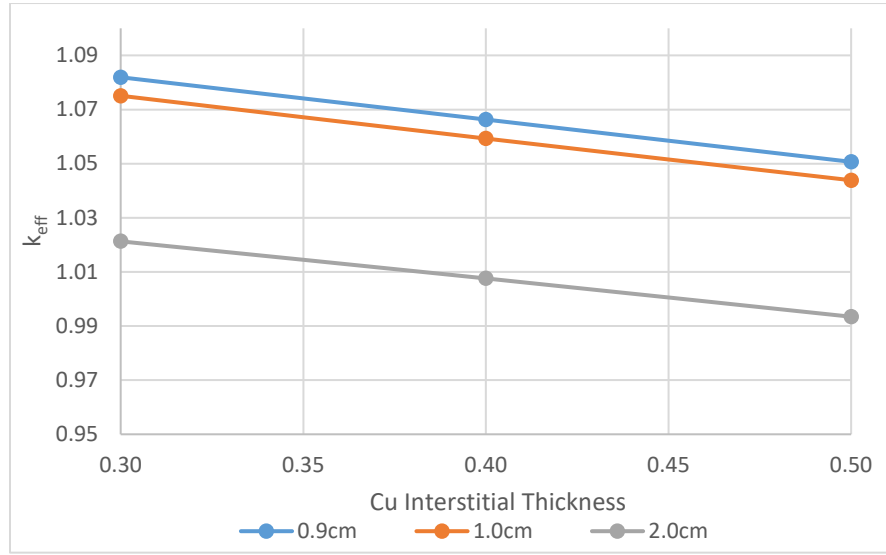


Figure B.1: k_{eff} vs. Cu interstitial thickness for SiC thickness of 0.9, 1.0, and 2.0cm. All simulations include 5 units and a 30cm Cu reflector

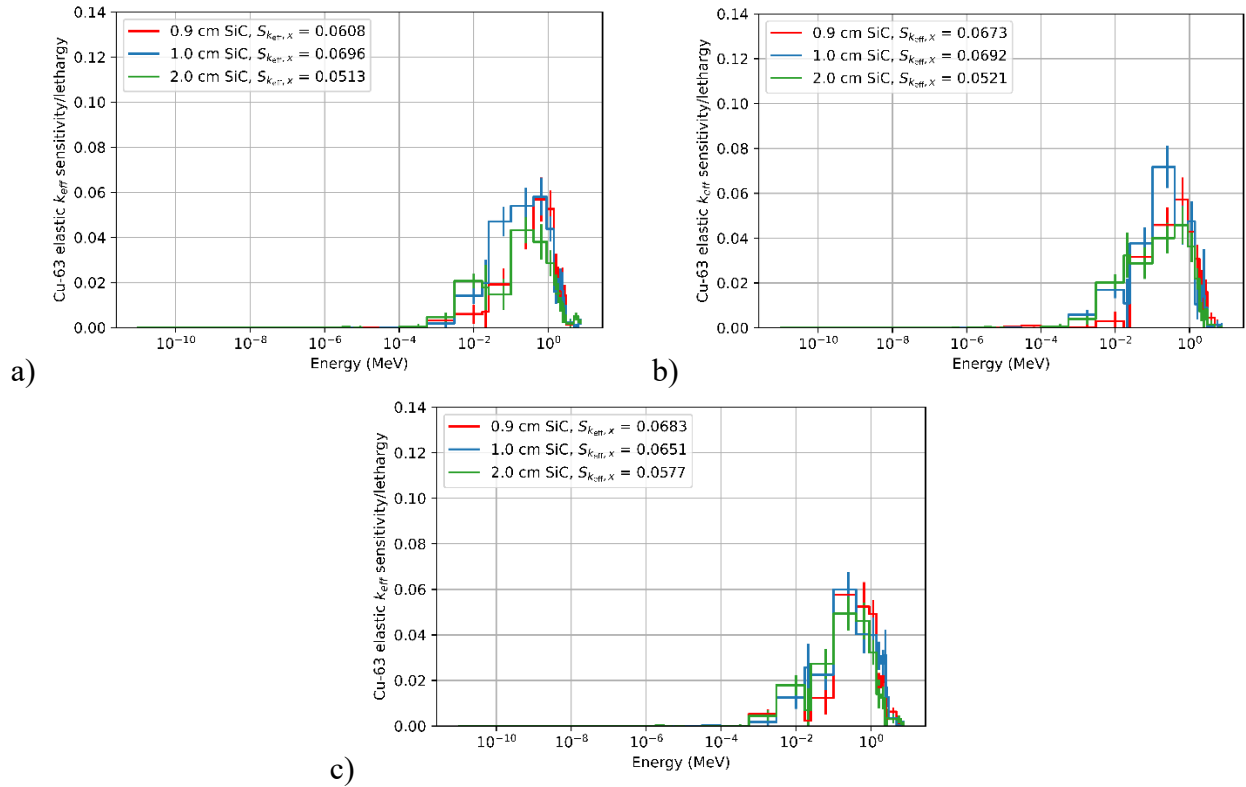


Figure B.2: ^{63}Cu elastic scattering sensitivities for configurations with 0.9 – 2.0cm SiC interstitial thickness and Cu interstitial thicknesses: a) 0.3cm, b) 0.4cm, and c) 0.5cm. Configurations only include 5 units and a 30cm Cu reflector.

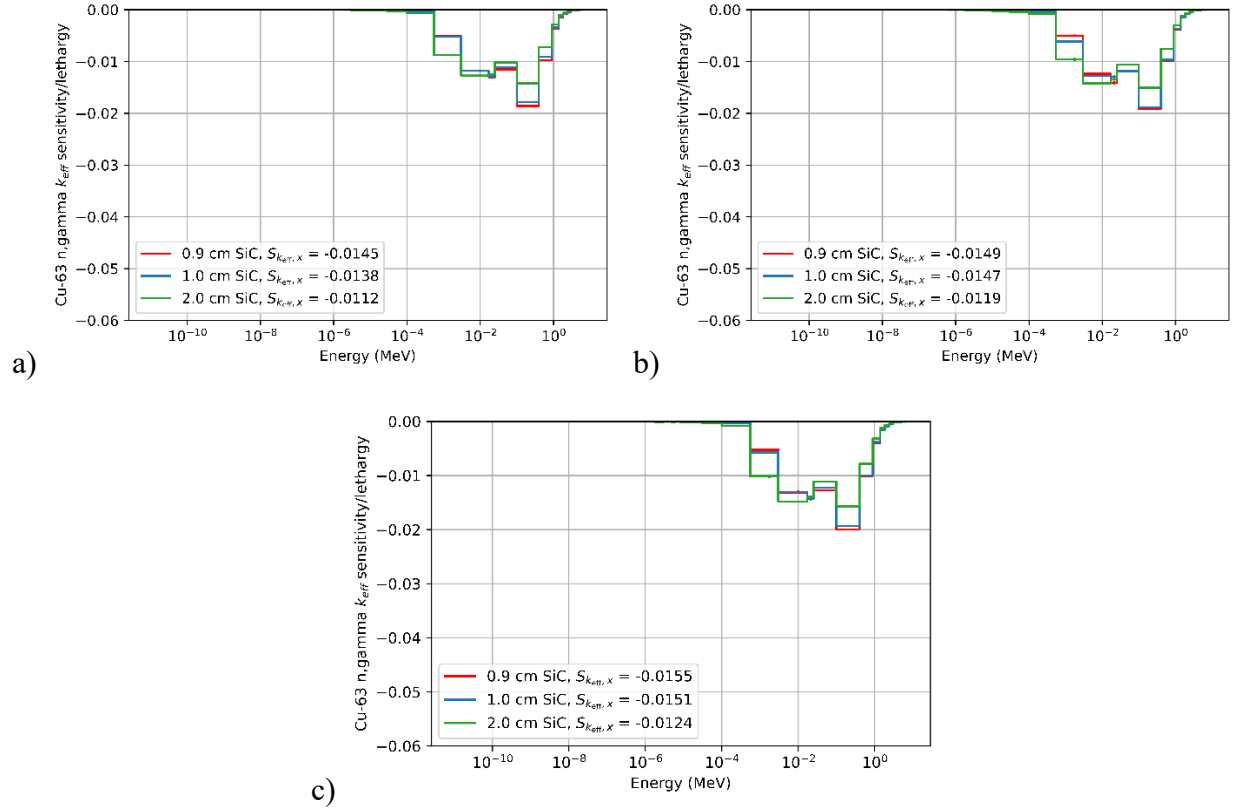


Figure B.3: ^{63}Cu (n, γ) sensitivities for configurations with 0.9 – 2.0cm SiC interstitial thickness and Cu interstitial thicknesses: a) 0.3cm, b) 0.4cm, and c) 0.5cm. Configurations only include five units and a 30cm Cu reflector.

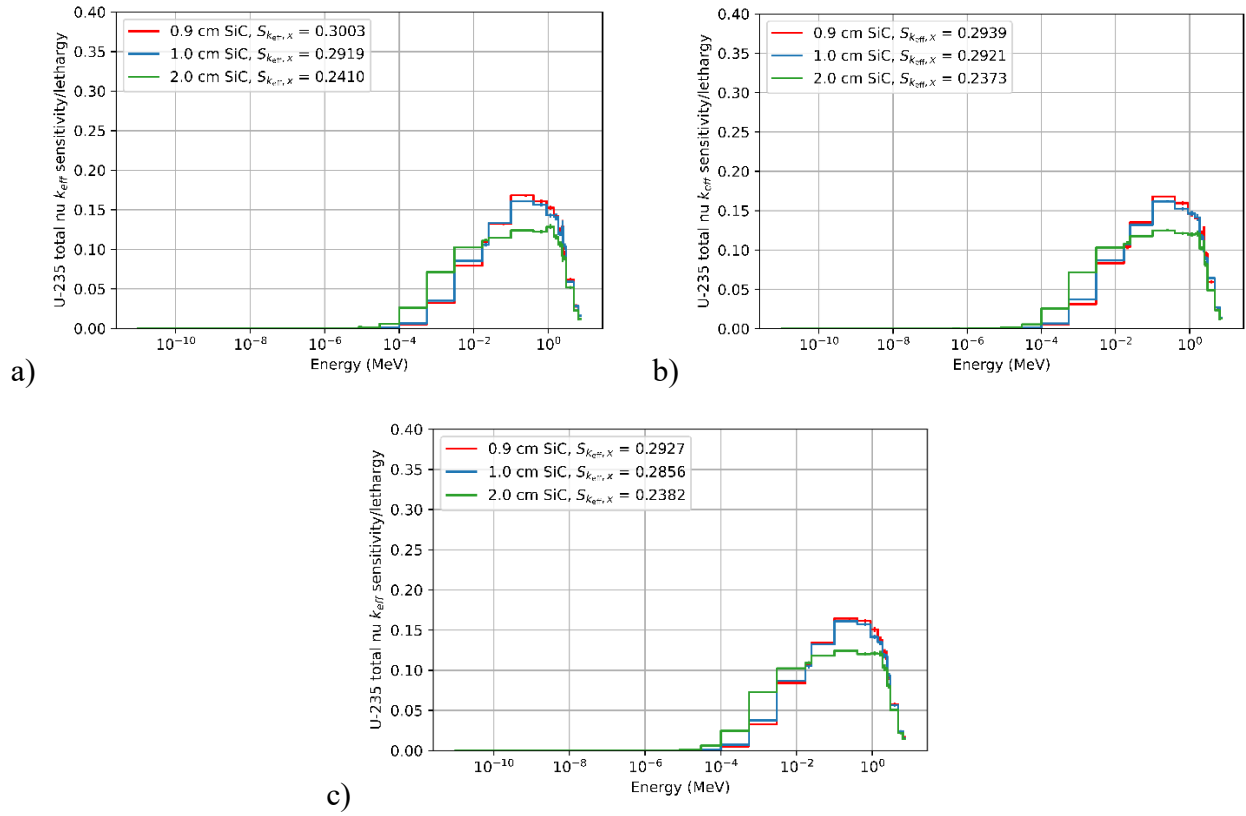


Figure B.4: ^{235}U total nu sensitivities for configurations with 0.9 – 2.0 cm SiC interstitial thickness and Cu interstitial thicknesses: a) 0.3 cm, b) 0.4 cm, and c) 0.5 cm. Configurations only include five units and a 30 cm Cu reflector.

APPENDIX C: SILICON DIOXIDE SENSITIVITY PLOTS

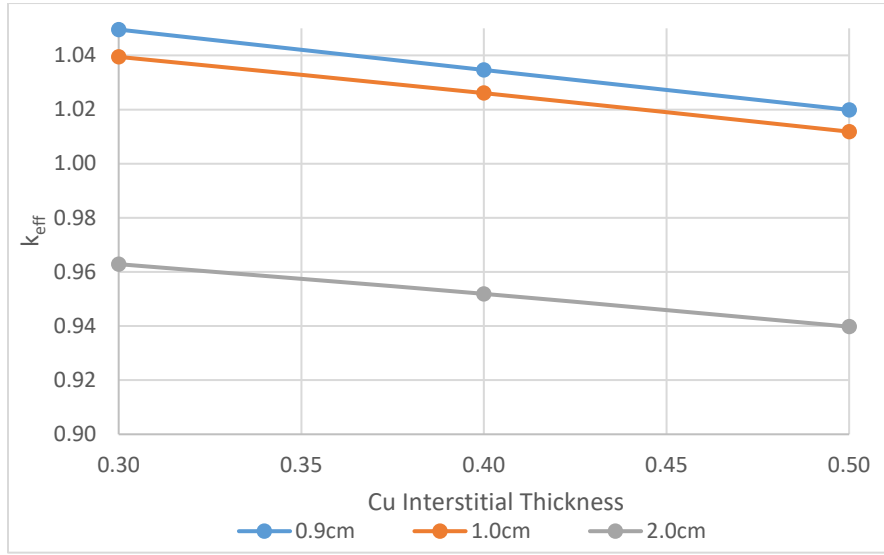


Figure C.1: k_{eff} vs. Cu interstitial thickness for SiO₂ thickness of 0.9, 1.0, and 2.0cm. All simulations include 5 units and a 30cm Cu reflector

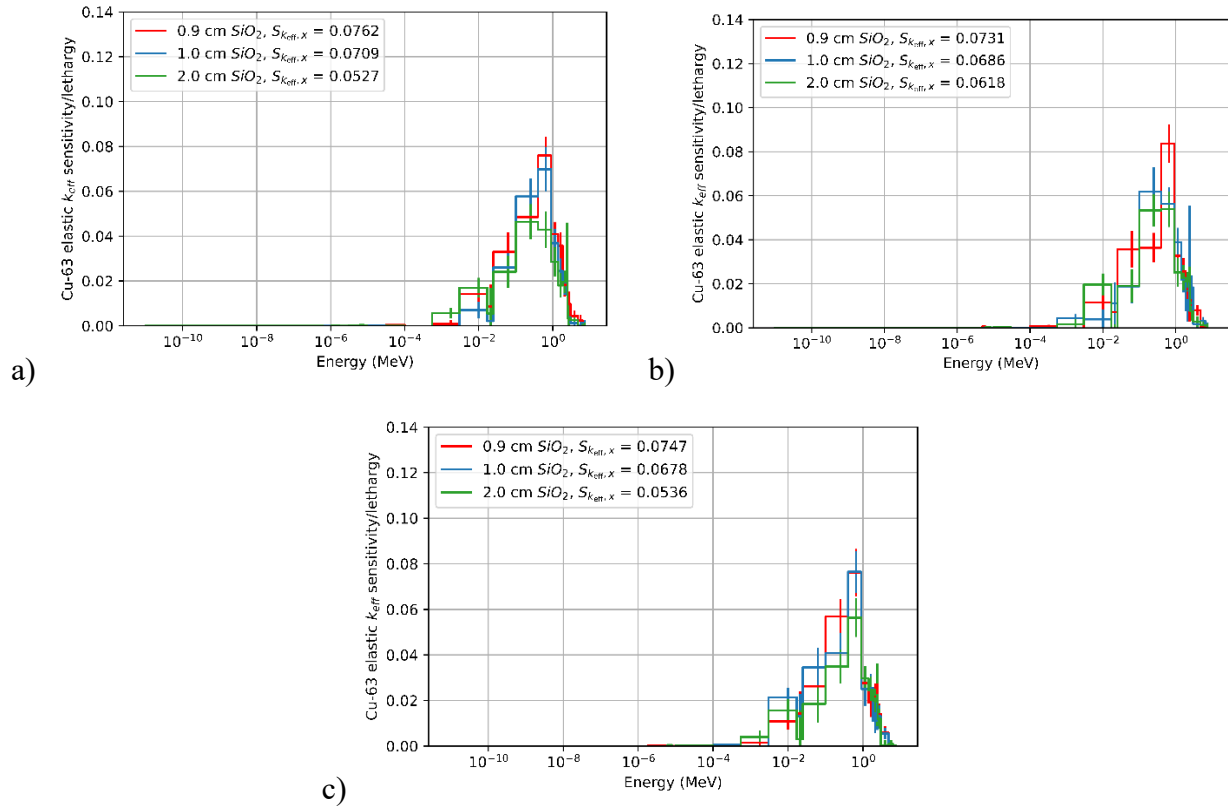


Figure C.2: ⁶³Cu elastic scattering sensitivities for configurations with 0.9 – 2.0cm SiO₂ interstitial thickness and Cu interstitial thicknesses: a) 0.3cm, b) 0.4cm, and c) 0.5cm. Configurations only include 5 units and a 30cm Cu reflector.

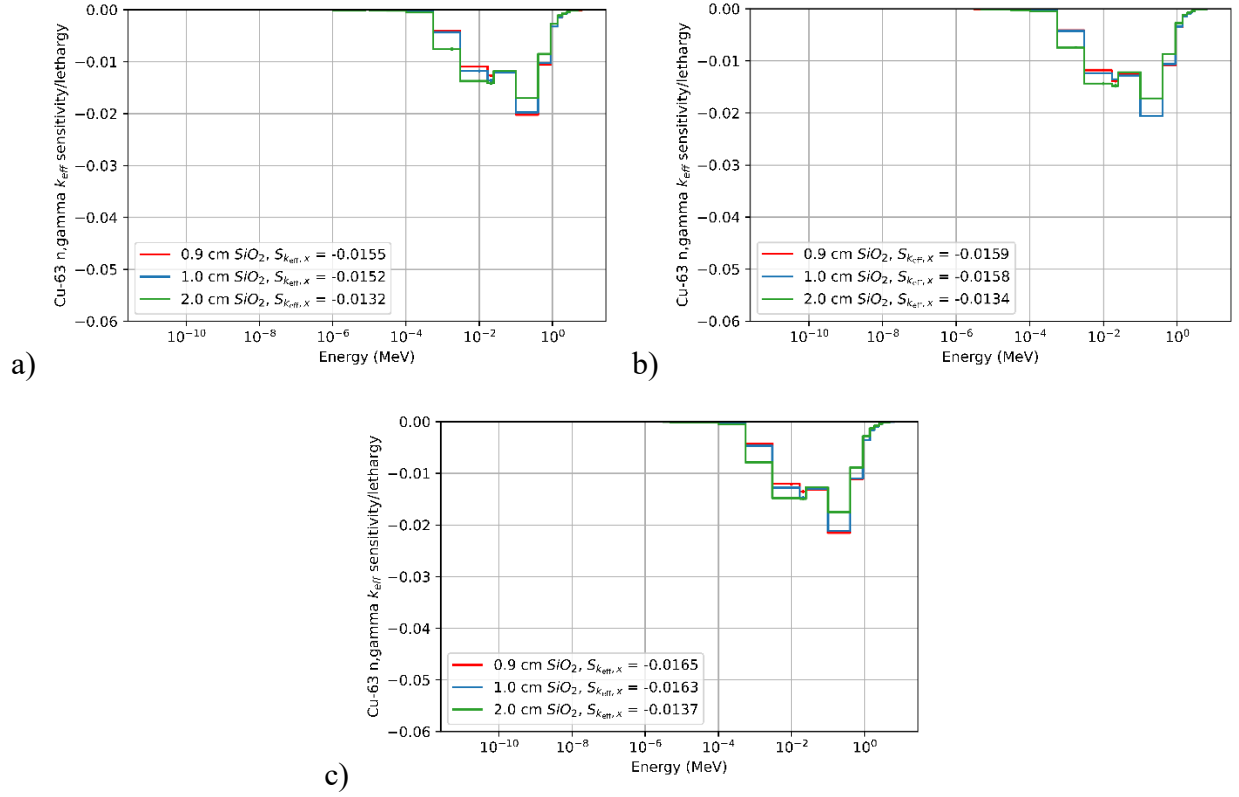


Figure C.3: ^{63}Cu (n, γ) sensitivities for configurations with 0.9 – 2.0cm SiO₂ interstitial thickness and Cu interstitial thicknesses: a) 0.3cm, b) 0.4cm, and c) 0.5cm. Configurations only include five units and a 30cm Cu reflector.

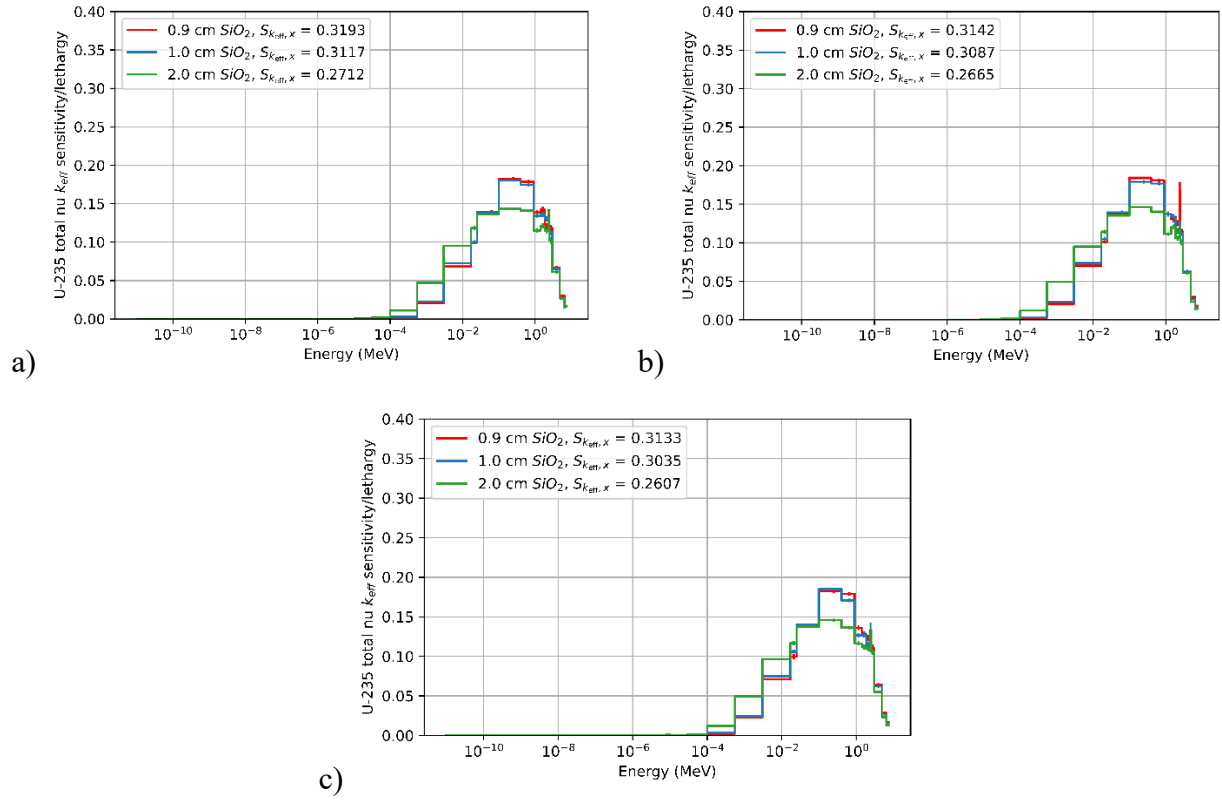


Figure C.4: ²³⁵U total nu sensitivities for configurations with 0.9 – 2.0 cm SiO₂ interstitial thickness and Cu interstitial thicknesses: a) 0.3 cm, b) 0.4 cm, and c) 0.5 cm. Configurations only include five units and a 30 cm Cu reflector.

APPENDIX D: SAMPLE MCNP INPUT FOR BASE

This input deck is a sample of the base input for a 0.3cm Cu interstitial thickness with a 30cm Cu reflector and 5 units.

c Generic Input

c

c Cell cards

```
10 1 -8.96 -601 100 -101 IMP:N=1
11 10 -18.39 -601 101 -102 IMP:N=1
12 1 -8.96 -601 102 -103 IMP:N=1
13 1 -8.96 -601 103 -104 IMP:N=1
14 10 -18.39 -601 104 -105 IMP:N=1
15 1 -8.96 -601 105 -106 IMP:N=1
16 1 -8.96 -601 106 -107 IMP:N=1
17 10 -18.39 -601 107 -108 IMP:N=1
18 1 -8.96 -601 108 -109 IMP:N=1
19 1 -8.96 -601 109 -110 IMP:N=1
20 10 -18.39 -601 110 -111 IMP:N=1
21 1 -8.96 -601 111 -112 IMP:N=1
22 1 -8.96 -601 112 -113 IMP:N=1
23 10 -18.39 -601 113 -114 IMP:N=1
24 1 -8.96 -601 114 -115 IMP:N=1
500 15 -8.96 601 -602 100 -115 IMP:N=1
501 15 -8.96 -602 -501 115 IMP:N=1
502 15 -8.96 -602 500 -100 IMP:N=1
600 0 602 IMP:N=0
601 0 -602 -500 IMP:N=0
602 0 -602 501 IMP:N=0
```

c Surface cards

```
100 PZ 0.0000
101 PZ 0.3000
102 PZ 0.5997
103 PZ 0.8997
104 PZ 1.1997
105 PZ 1.4994
106 PZ 1.7994
107 PZ 2.0994
108 PZ 2.3992
109 PZ 2.6992
110 PZ 2.9992
111 PZ 3.2989
112 PZ 3.5989
113 PZ 3.8989
114 PZ 4.1986
115 PZ 4.4986
```

500 PZ -30.0000
501 PZ 34.4986
601 CZ 26.6700
602 CZ 56.6700

c Data Cards

KSEN1 xs

rxn = +2 +4 -6 +16 102 103 104 105 106 107 -7 -1018

erg =

1.0000e-11 3.0000e-09 7.5000e-09 1.0000e-08 2.5300e-08 3.0000e-08
4.0000e-08 5.0000e-08 7.0000e-08 1.0000e-07 1.5000e-07 2.0000e-07
2.2500e-07 2.5000e-07 2.7500e-07 3.2500e-07 3.5000e-07 3.7500e-07
4.0000e-07 6.2500e-07 1.0000e-06 1.7700e-06 3.0000e-06 4.7500e-06
6.0000e-06 8.1000e-06 1.0000e-05 3.0000e-05 1.0000e-04 5.5000e-04
3.0000e-03 1.7000e-02 2.5000e-02 1.0000e-01 4.0000e-01 9.0000e-01
1.4000e+00 1.8500e+00 2.3540e+00 2.4790e+00 3.0000e+00 4.8000e+00
6.4340e+00 8.1873e+00 2.0000e+01

c Material Cards

c Fuel

M10 92235.00c 0.93

92238.00c 0.07

c Reflector

M15 29063.00c 0.6917

29065.00c 0.3083

c Moderator 1

M1 29063.00c 0.6917

29065.00c 0.3083

c kcode

KCODE 10000 1.0 100 600

KSRC 0.0 0.0 0.4499

0.0 0.0 1.3496

0.0 0.0 2.2493

0.0 0.0 3.1490

0.0 0.0 4.0487

APPENDIX E: SAMPLE MCNP INPUT FOR BASE+

This input deck is a sample of the base+ input for a 1.0cm Cu interstitial thickness and a 0.3cm polyethylene thickness with a 30cm Cu reflector and 5 units.

c Generic Input

c

c Cell cards

```
10  2  -8.96 -601  100 -101 IMP:N=1
11  1  -0.93 -601  101 -102 IMP:N=1
12  10  -18.39 -601  102 -103 IMP:N=1
13  1  -0.93 -601  103 -104 IMP:N=1
14  2  -8.96 -601  104 -105 IMP:N=1
15  2  -8.96 -601  105 -106 IMP:N=1
16  1  -0.93 -601  106 -107 IMP:N=1
17  10  -18.39 -601  107 -108 IMP:N=1
18  1  -0.93 -601  108 -109 IMP:N=1
19  2  -8.96 -601  109 -110 IMP:N=1
20  2  -8.96 -601  110 -111 IMP:N=1
21  1  -0.93 -601  111 -112 IMP:N=1
22  10  -18.39 -601  112 -113 IMP:N=1
23  1  -0.93 -601  113 -114 IMP:N=1
24  2  -8.96 -601  114 -115 IMP:N=1
25  2  -8.96 -601  115 -116 IMP:N=1
26  1  -0.93 -601  116 -117 IMP:N=1
27  10  -18.39 -601  117 -118 IMP:N=1
28  1  -0.93 -601  118 -119 IMP:N=1
29  2  -8.96 -601  119 -120 IMP:N=1
30  2  -8.96 -601  120 -121 IMP:N=1
31  1  -0.93 -601  121 -122 IMP:N=1
32  10  -18.39 -601  122 -123 IMP:N=1
33  1  -0.93 -601  123 -124 IMP:N=1
34  2  -8.96 -601  124 -125 IMP:N=1
500  15  -8.96 601 -602  100 -125 IMP:N=1
501  15  -8.96 -602 -501  125 IMP:N=1
502  15  -8.96 -602 500 -100 IMP:N=1
600  0  602 IMP:N=0
601  0  -602 -500 IMP:N=0
602  0  -602 501 IMP:N=0
```

c Surface cards

```
100  PZ  0.0000
101  PZ  1.0000
102  PZ  1.3000
103  PZ  1.5997
104  PZ  1.8997
105  PZ  2.8997
```

106	PZ	3.8997
107	PZ	4.1997
108	PZ	4.4994
109	PZ	4.7994
110	PZ	5.7994
111	PZ	6.7994
112	PZ	7.0994
113	PZ	7.3992
114	PZ	7.6992
115	PZ	8.6992
116	PZ	9.6992
117	PZ	9.9992
118	PZ	10.2989
119	PZ	10.5989
120	PZ	11.5989
121	PZ	12.5989
122	PZ	12.8989
123	PZ	13.1986
124	PZ	13.4986
125	PZ	14.4986
500	PZ	-30.0000
501	PZ	44.4986
601	CZ	26.6700
602	CZ	56.6700

c Data Cards

KSEN1 xs

rxn = +2 +4 -6 +16 102 103 104 105 106 107 -7 -1018

erg =

1.0000e-11	3.0000e-09	7.5000e-09	1.0000e-08	2.5300e-08	3.0000e-08
4.0000e-08	5.0000e-08	7.0000e-08	1.0000e-07	1.5000e-07	2.0000e-07
2.2500e-07	2.5000e-07	2.7500e-07	3.2500e-07	3.5000e-07	3.7500e-07
4.0000e-07	6.2500e-07	1.0000e-06	1.7700e-06	3.0000e-06	4.7500e-06
6.0000e-06	8.1000e-06	1.0000e-05	3.0000e-05	1.0000e-04	5.5000e-04
3.0000e-03	1.7000e-02	2.5000e-02	1.0000e-01	4.0000e-01	9.0000e-01
1.4000e+00	1.8500e+00	2.3540e+00	2.4790e+00	3.0000e+00	4.8000e+00
6.4340e+00	8.1873e+00	2.0000e+01			

c Material Cards

c Fuel

M10 92235.00c 0.93

92238.00c 0.07

c Reflector

M15 29063.00c 0.6917

29065.00c 0.3083

c Moderator 1

M1 1001.00c 8.24145E-02

1002.00c 1.23640E-05
6012.00c 4.12154E-02
MT1 h-poly.40t
c Moderator 2
M2 29063.00c 0.6917
29065.00c 0.3083
c kcode
KCODE 10000 1.0 100 600
KSRC 0.0 0.0 1.4499
0.0 0.0 4.3496
0.0 0.0 7.2493
0.0 0.0 10.1490
0.0 0.0 13.0487